Controlled structure and hydrophilic property of polymethylhydrosiloxane thin films attached on silicon support and modified with phosphorylcholine group

Thierry Thami, Lara Tauk, Valérie Flaud

Highlights:

- Functionalization of hydroxylated substrate with a matrix surface rich in SiH group
- Surface of high density of phosphorylcholine group for biomedical applications
- Elaboration of functional film with cured polymethyldroxysiloxane in two steps
- Controlled structure and functionality of T-crosslinked polysiloxane network
- Evidence of 2:1 (Si:phospholipid) hydrosilylation adducts with linoleoyl chains

Controlled structure and hydrophilic property of polymethylhydrosiloxane thin films attached on silicon support and modified with phosphorylcholine group

Thierry Thami,[a,*] Lara Tauk,[a,1] Valérie Flaud[b]

[a]Institut Européen des Membranes, IEM, UMR-5635, Université de Montpellier, ENSCM, CNRS Place Eugène Bataillon, 34095 Montpellier cedex 5, FRANCE

[b]XPS Technological platform, Institut Charles Gerhardt, ICG, Université de Montpellier, Place Eugène Bataillon, 34095 Montpellier cedex 5, FRANCE

*Corresponding author. *E-mail addresses*: thierry.thami@umontpellier.fr (T. Thami), ltauk@ndu.edu.lb (L. Tauk), valerie.flaud@umontpellier.fr (V. Flaud).

[1]Present address at: Department of Sciences, Faculty of Natural and Applied Science, Notre Dame University (Louaize), Zouk Mosbeh, Lebanon.

Abstract

Thin films of crosslinked polymethylhydrosiloxane (PMHS) are grafted on silica using sol-gel process allowing subsequent coupling of molecules by hydrosilylation grafting to Si–H groups. The aim was to fabricate stable polysiloxane film on solid supports with well-characterized functionalities and surface properties for various applications. The pristine PMHS surface was modified with phosphorylcholine group by reaction at room temperature or 40 °C catalyzed by Karsted's catalyst with a phospholipid molecule containing linoleoyl chains to form hydrophilic surfaces as a model. The purpose was to characterize precisely the structure and composition of virgin and treated PMHS films in relation with the wetting properties by using IR and X-ray photoelectron spectroscopies (XPS). The surface properties were studied by pure water contact

angle measurements in air by using sessile drops and captive bubbles, atomic force microscopy, and scanning electron microscopy. The modified surfaces are highly hydrophilic with contact angle varying from 40 to 0°. Analysis of the composition of the surface showed that the reaction of linoleoyl chains gives the 2:1 (Si:phospholipid) hydrosilylation adducts resultant from one fold addition of methylhydrosilane on each linoleoyl chain. The graft yield in terms of molecular percentage determined by XPS in various conditions was correlated in good agreement with wetting properties and previous protein adsorption measurements for comparison purpose.

Keywords : Polymethylhydrosiloxane; Crosslinking; Chemical modification; Grafting; Hydrosilylation; Hydrophilic surface; Structure-property relation; X-ray photoelectron spectroscopy.

1. Introduction

The control of structure and composition of tailored interfaces between polymers and a surrounding medium are of great importance to improve interfacial properties in a number of applications. Examples are given by surfaces of biomaterials that control the wetting and the absorption of proteins which is required in implanted medical devices [1,2], biosensors [3,4], contact lenses [5], lab-on-chips devices [6], substrates for enzyme-linked immunosorbent assays (ELISA) [7] and blood compatible materials [8,9]. Other applications in which functional polymer plays an active role at the interfaces include membrane separation [10,11], adhesion [12] and smart surfaces with sensing properties [13,14]. However, it is still a challenge to fabricate polymer layers on solid surfaces with well-defined relationship between structures and properties, that are stable, uniform, continuously defect free, and that allow further chemical modification with molecules or various functionalities.

Our goal was to tailor polymer thin film grafted by covalent bonding with alkoxysilane reagents to afford a stable structure with strong adhesion to the substrate [15]. We developed recently a method for surface modification of solid substrates by chemical attachment of sol-gel cured polymethylhydrosiloxane (PMHS) polymer network containing SiH functionalities [16]. Compared with the room temperature vulcanization process [17], this method offers the advantage of a one-step polymerization process that gives continuous and homogeneous thin films of controlled thicknesses in the micrometer range. Moreover, the mechanical properties of the PMHS thin films can be easily tuned by sol-gel formulation [16]. This process results in a biocompatible and homogenous silicone platform containing reactive SiH groups with controlled flexibility. The introduction of siloxane building blocks with Si–H bonds would be a suitable synthetic approach for the decoration of surfaces with functional groups. The reactive methyl

hydrosiloxane Si–H polymers [18] of structure [–OSi(H)Me–]/D^H can serve as chemical links to covalently attach the desired functionality through well-known catalytic hydrosilylation reaction *via* an alkene precursor [17–23]. Hydrosiloxanes are useful for the preparation of many organic/inorganic hybrid materials [24–26] and polymers with alkyl chains exhibiting self-assembly [27,28] using the reactivity of the Si−H bonds. We previously reported the fabrication of chemical sensors by surface modification of silica substrates with PMHS films for the detection of nitroaromatic compounds [29] or metal ions [30]. Similarly, the trend of reactivity of sol-gel cured PMHS films of various crosslinks densities was first studied by using terminal 1-alkenes with Karstedt's catalyst [31]. Hydrosylilation results in the formation of hydrolytically stable Si–C bonds. This is essential for polymer-based chemical sensors in order to avoid molecule leakage into the medium and inefficient analyses.

In the present work, we were interested in preparing smooth polysiloxane thin films on silicon wafer as a model to form surfaces with controllable structure and hydrophilic properties targeted for anti-biofouling applications. The main parameters for the design of protein resistance surfaces are related to the hydrophilic nature of the functionalized material, the density and accessibility of the hydrophilic groups [8]. The formation of electrically neutral surface [32] and the surface topography can also control the interactions with proteins [33]. One of the most effective approach for preventing the adhesion of protein involves the functionalization of surfaces with polymer bearing very hydrophilic phosphorylcholine (PC) head groups [34–37]. In recent years, different strategies have been developed to allow the grafting of PC-based polymers or PC containing molecules on various substrates and to afford stable, homogenous and PC-rich interfaces with long term protein repellent behavior. Surface graft polymerization incorporating PC moieties in particular with 2-methacryloxyethyl phosphoryl choline (MPC) monomer has

been used to covalently attach poly-(MPC) to silica [38–40] or polymers [41–48] through conventional free-radical polymerization initiated by various methods. Self-assembled monolayers using alkane-thiol [49,50] or disulfide [51,52] molecules containing the PC head group were prepared on gold surfaces. Grafting PC on solid surfaces has also been achieved using siloxane chemistry through coupling of phospholipid derivatives with an aminosilane coupling agent on a silica surface such as glass or silicon wafers [53,54]. PC derivatives with dimethylchlorosilane were synthezised to coat glass by covalent bonding [55,56]. Silanated zwiterrionic PC molecules were recently prepared by the hydrosilylation reaction of the MPC monomer with triethoxysilane before covalent fixation on titanium alloy [57]. A crosslinkable coating from a PC-based polymer having pendent trimethoxysilane group has been prepared to improve the stability of the film and the possibility of anchoring the polymer to substrate [58]. However, chemical transformation of the phosphorycholine-containing molecule was necessary to obtain the polymerizable or functional group permitting covalent bonding to the surface. These methods have a great disadvantage: they present some difficulties in the reproductibility of the process of surface modification, in particular in the case of the polymerization process of the MPC monomer. Alternative methods have been recently developed by use of active surfaces with electrically switchable hydrophobic/hydrophilic wettability targeted to prevent bacterial attachment and biofilm formation [59,60].

Surfaces of PMHS modified with zwitterionic PC groups have also been investigated for protein resistance [61, 62]. The surfaces were prepared by grafting a natural phospholipid precursor bearing unsaturated fatty chains to PMHS films on glass or silicon. Additionally, very few studies have reported the hydrosilylation of unsaturated fatty acid derivatives [27, 63–70]. The catalytic hydrosylilation process to PMHS films gave surfaces of high densities of phospholipid

that are highly hydrophilic and strongly resistant to several proteins [61, 62] (fibrinogen adsorption < 5 ng/cm^2) in comparison with other zwitterionic materials (sulfobetaine, carboxybetaine) [71,72]. However, there is no report to control hydrophilicity and consequently the adsorption of proteins for the PC-silicone surfaces prepared by hydrosilylation grafting to PMHS.

We hereby propose to analyze the relationships between the chemical structure and hydrophilic properties of the phospholipid functionalized PMHS polymer in relation with the hydrosilylation procedure used for its surface modification. The main goal was to get a description, as precise as possible, of the structure of these gels before and after reaction. The structural characteristics of the films were investigated by X-ray photoelectron spectroscopy (XPS) and infrared spectroscopy (IR). The surfaces properties were examined by water contact angle (WCA) measurements in air, atomic force microscopy (AFM) and scanning electron microscopy (SEM). The surface wetting behavior and protein adsorption are finally discussed and correlated in terms of phospholipid grafting density in relation with the proposed chemical structure.

2. Experimental details

2.1. Chemicals

Both precursors methyldiethoxysilane $HSi(CH_3)(OCH_2CH_3)_2$ (DH) and triethoxysilane $HSi(OCH_2CH_3)_3$ (TH), and the sol-gel catalyst trifluoromethanesulfonic acid CF_3SO_3H were purchased from Aldrich and used as received. Water for substrate cleaning was obtained from a Milli-Q water purification apparatus (Millipore). Absolute ethanol for sol–gel synthesis was of synthesis grade purity. Toluene for thin film hydrosilylation was dried and distilled with calcium hydride before use. The platinum complex [Pt_2(*sym*-tetramethyldivinyldisiloxane)$_3$] in xylene (platinum concentration *ca.* 0.1 M assuming 2.4 % (w) Pt), also known as Karstedt's catalyst,

was purchased from Aldrich. 1,2-dilinoleoyl-sn-glycero-3-phosphorylcholine (18:2 Cis) (PL) was purchased from AvantiPolarLipids.

2.2. Thin films preparation

2.2.1. Substrate cleaning and activation

Silicon wafers Si(100) (ACM, France) cut into square strips of 2 × 2 cm^2 were used as substrates for spin-coating deposition. To bond covalently the PMHS thin films to native oxide silica (thickness ~ 2 nm) of silicon wafer, the substrates were first cleaned and activated with "piranha" solution using the previously described procedure [16]. Caution: 'piranha' solution must be handled extremely carefully.

2.2.2. Synthesis of crosslinked PMHS films

PMHS thin films of various crosslinking densities (30, 15 and 5 mol % TH) were prepared at room temperature by sol–gel polymerization of DH:TH sol mixtures deposited by spin-coating on silicon wafer (100) substrates freshly activated by "piranha" solution. The procedure is briefly summarized as follows [30, 31]. The mixture DH/TH of monomers (4.0 M in EtOH; molar ratio $[EtOH]/[Si] = 1$) was polymerized with hydrolysis ratio $h = [H_2O]/[SiOEt] = 0.5$. Trifluoromethanesulfonic acid CF_3SO_3H (1.0 M in absolute ethanol) was used as catalyst (0.5 mmol/mol of monomers). The freshly activated substrate was purged (2 min) in the spin-coater (Spin150, SPS Europe) under a stream of nitrogen (2 L/min) to avoid air moisture. The resulting clear sol was allowed to age for about 30 minutes with magnetic stirring before spin-coating deposition to give a fully crosslinked [16] thin film (~ 0.5 μm). For all samples, the speed of rotation was 4000 rpm (spin acceleration 2000 rpm/s) and the rotation time 30 s. The coated samples were finally cured at 110 °C in an oven for ten minutes. This procedure gave PMHS spin-coated films of reproducible homogeneity and thickness as measured by IR

spectroscopy (Section 2.3.2). The PMHS samples of various crosslinking densities were analyzed after curing.

2.2.3. Hydrosilylation of PMHS films with phospholipid

2.2.3.1. Casting

The hydrosilylation reaction between the dilinoleoyl phospholipid and the PMHS Si–H function was performed in air by casting a toluene solution of phospholipid in the presence of Karstedt's catalyst onto the substrate bearing 5 % lightly crosslinked PMHS film. 20 mg of the reactant 1,2-dilinoleoyl-sn-glycero-3-phosphorylcholine (18:2 Cis) were dissolved in 1 mL of dry toluene under argon to avoid air moisture and 2 µL of the Pt-xylene solution were added. The samples were covered with 200 µL of phospholipid solution (25.6 mM) at room temperature and were kept for about one hour under a cap, and then left in open air to allow total evaporation of toluene. The phospholipid compound was in 1.5-fold excess with respect to available hydrogenosilane SiH group for a thin crosslinked PMHS film coated on silicon wafer or glass (0.5 µm thickness, 2 cm × 2 cm) assuming the density of the PMHS layer is about 1 g/mL. To finish the reaction, the sample was then heated for an additional curing time (1 to 15 hours) at 40 °C in a thermostated box (Relative Humidity 12 % ± 2 %) to protect the reaction from ambient moisture.

2.2.3.2. Immersion

The hydrosilylation reaction was also performed with 1.5-fold excess of PL over SiH group by placing 5 % crosslinked PMHS film anchored on wafer in 1.6 ml of phospholipid solution (3.2 mM) prepared as follows: 20 mg of PL were dissolved in 8 mL of dry toluene under argon with additional 7 µL of the Karstedt Pt-catalyst. Typically, various samples were immersed for 1 to 6 hours without stirring at room temperature.

2.2.3.3. Washing procedure

For both methods, the PL modified samples were denoted as PL-PMHS. They were rinsed after reaction successively in different toluene/chloroform mixtures from 100/0 to 0/100 (% Vol.) with a gap of 20 % and dried under a stream of argon. The samples were then rinsed with water (2 h) to remove any physisorbed material, and finally dried under a stream of argon. Freshly prepared PL-PMHS surfaces were analyzed to avoid pollutants contamination.

2.3. Characterization techniques

2.3.1. Infrared spectroscopy

The Fourier-transform infrared (FTIR) spectroscopy analyses were carried out on a Nicolet Nexus FTIR spectrometer. Transmission FTIR spectra were recorded in the 4000–400 cm^{-1} range with a resolution of 1 cm^{-1} and 32 scans to obtain qualitative and quantitative informations about yield of hydrosilylation reaction. A background spectrum was recorded using a piece of bare unmodified silicon wafer in air. Calculations for the films after reaction were based on CH_2 absorption with an accuracy of ± 5% neglecting SiH content (~ 0%) because 32 scans analysis was not enough to provide an accurate measurement.

2.3.2. Thickness measurements of virgin PMHS

The thickness (e) of virgin PMHS film (5% crosslinked) deposited on silicon wafer was measured by FTIR spectroscopy from the absorbance of the Si–H peak at 2169 cm^{-1} according to the Beer–Lambert law $A_{2169} = \alpha_{SiH} \times e$. The absorption coefficient $\alpha_{SiH} = \varepsilon_{SiH} \times [SiH] = 0.27\ \mu m^{-1}$ was calibrated for thin film samples of 200 nm thick for which independent thickness was easily measured using ellipsometry (Accuracy of ± 5%). Ellipsometry was achieved on a Horiba Jobin Yvon PZ2000 ellipsometer equipped with a 632.8 nm He-Ne laser with a spot size of 2 mm. The angle of incidence was 70.0°. The thickness of the silicon oxide

layer of about 2 nm was measured separately assuming the refractive index n = 1.457 for SiO_2 and $n = 3.871 - 0.16i$ for silicon, and for PMHS coatings we used a fixed refractive index of n = 1.40 ± 0.02 [16,31].

2.3.3. X-ray photoelectron spectroscopy

XPS data were obtained on an ESCALAB 250 (Thermo Electron, UK) spectrophotometer using Al Kα (1486.6 eV) irradiation source (15 kV, 100 W). The photoelectrons were analyzed at normal incidence of the sample surface. The spot size was approximately 400 μm^2. The composition corresponds to depths of 5–10 nm. Survey scans (0–1350 eV) at low resolution were performed to identify the constitutive elements. The peaks were fitted with Gauss–Lorentz curves with the theoretical sensitivity factors reported by Scofield [73]. Si_{2p} doublets were considered in the fitting process of the Si_{2p} core level [74,75]. A charge correction was applied to set the binding energy scale. The spectra were calibrated using the hydrocarbon contaminant or alkane C_{1s} peak at 284.8 eV. In both cases, the peak of Si-$\underline{C}H_3$ was found at a binding energy of 284.0 eV in agreement with PDMS polymer [76] at 284.4 eV.

2.3.4. Atomic force microscopy

AFM experiments were performed using a Dimension 3100 microscope equipped with a Nanoscope IIIa controller system (Digital Instruments, Veeco Metrology Group). AFM images were obtained by scanning in tapping mode under air ambient conditions using silicon SPM probes (stiffness k ≈ 2 N/m, resonance frequency of 67 kHz, pointe probeplus, Nanosensors). All images were analyzed using data-processing software Gwyddion (Version 2.54).

2.3.5. Scanning electron microscopy

SEM pictures of cross section and thickness of the films were obtained with a Hitachi S-4800 instrument operating at an accelerating voltage of 2 kV, and with different magnifications of 18k × and 40k ×.

2.3.6. Water contact angle measurement

Air captive bubble and sessile drop WCAs were measured (Contact angle meter, GBX, France) by applying to the surface respectively, an air bubble of about 8 µL in water, and a 3 µL water droplet in ambient air. The air captive bubble WCAs discussed are relative to the complement angle (θ) to 180° through the liquid [77]. The receding and advancing WCAs were measured using the injection and the withdrawn of a 5 µL water droplet by using a motor-driven syringe at constant speed of 0.5 µl/min. WCAs were calculated by an automated polynomial fitting method using computerized image analysis (Visiodrop, GBX).

3. Results and discussion

3.1. Synthesis of the PMHS and PL-PMHS films

3.1.1. Crosslinked PMHS films

A reactive polymethylhydrosiloxane PMHS polymer crosslinked by the sol-gel reaction of hydrogenosilane precursors was prepared in the first step (Scheme 1a). PMHS films were synthesized on silicon wafer at room temperature by acid-catalyzed polymerization of a sol-gel mixture of methyldiethoxysilane/triethoxysilane (DH/TH) using the spin-coating procedure giving fully crosslinked network. Neglecting a small amount of remaining cycles in the 3D network, the resulting surface-attached 3D polymer network can be characterized by the average number of monomer units [–OSi(H)CH_3–] in PMHS segment between crosslink subunits $SiHO_{3/2}$:

$$N = 2\alpha/3(1-\alpha) \quad (1)$$

where $\alpha/(1-\alpha)$ is the composition of DH/TH mixture. The soft PMHS material prepared with a small amount of TH additive (5 mol %) was used because polymer (3D-network) or multilayers of PMHS chains are created in such lightly crosslinked PMHS network with $N \sim 13$ from Eq. (1).

3.1.2. Phospholipid functionalized PL-PMHS films

The chemical grafting process is shown in Scheme 1b with the unsaturated phospholipid (PL) molecule bearing internal double bonds. The hydrosilylation reaction in the presence of Karstedt's platinum catalyst and air allows subsequent functionalization in PMHS layer by hydrosilylation of the SiH groups with one of the internal double bond of each linoleoyl chains. The hydrosilylation reaction was carried out using an excess of alkenes with respect to available SiH on a spin-coated PMHS thin film (Experimental details). Thus, the linoleoyl chain of phospholipid molecule could be connected to SiH groups by hydrosilylation in different polymethylhydrosiloxane layers at the interface by bridging the polysiloxane chains. In addition, the reaction of many linoleoyl chains may also increase the crosslinking density of the PMHS gel.

By anticipating XPS results (Section 3.3), we postulated that hydrosylilation of PL molecule may lead preferentially to the formation of the 2:1 (Si:PL) alkene adduct resultant from onefold addition of methylhydrosilane on each linoleoyl chain of PL molecule as sketched in boxed Scheme 1b. This reaction scheme is different from that proposed in our previous work where we assumed that all double bonds of PL have reacted with SiH to form 4:1 (Si:PL) adduct [61]. Indeed, Behr *et al*. [67, 68] showed that the reactivity of internal double bonds of unsaturated fatty acid ester such as methyl linoleate is lower than that of terminal double bond. Such a low reactivity of internal double bonds was also reported in the case of fatty amide [69] and

triacylglycerol [70] derivatives. The proposed reaction scheme supports the assumption that there is a conjugation of the two internal double bonds before hydrosilylation and migration of the remaining double bond in the product after reaction [67, 68]. The formation of a mixture of cis/trans isomers is also postulated as side reaction.

3.2. Infrared analysis

3.2.1. Characterization of virgin PMHS and functionalized PMHS films

The chemical structure of the obtained PMHS film before and after hydrosilylation by casting method was characterized by FTIR spectroscopy (Fig. 1a and b). The peak assignments are summarized in Table 1. From spectrum of virgin PMHS (Fig. 1a) to spectrum PL-PMHS (Fig. 1b), the strong absorption peaks of Si–H groups (2169 and 838 cm^{-1}) [16,78] almost vanished while that of C=O (1736 cm^{-1}), CH_2 (2856 and 2926 cm^{-1}) and PO (1090 and 1250 cm^{-1}) groups appeared. These observations seem to confirm the reaction of phospholipid molecules in PMHS film after hydrosilylation and solvent washing. The phosphate band ν(PO) in the phosphorylcholine subunit was found to overlap as shoulder peak at about 1090 cm^{-1} with the very strong SiOSi doublet of the PMHS matrix.

The grafting process of PL to the polysiloxane backbone is also evidenced by the modification of the single sharp band $\delta_s(SiCH_3)$ for PMHS which is split in PL-PMHS spectrum at 1271 cm^{-1} indicating clearly the appearance of new $\delta_s(SiCH)$ bands [31]. As no IR spectral evidence for any remaining C=C bonds was found in PL-PMHS film by comparison with spectrum of PL molecule (Fig. 1b and c), we can conclude that hydrogenation of the remaining unreacted double bonds occurred as an undesired side pathway [67,68,70] to give a saturated aliphatic grafted structure made of stearate-like chains. The remaining double bonds of grafted PL molecules can

react with SiH silane groups present onto PMHS film. To conclude, these FTIR data are consistent with the chemical structure for the PL-PHMS film sketched in Scheme 1b.

3.2.2. Reaction of PMHS with water

The evolution of transmission IR absorption spectra of PMHS films (~ 0.5 μm) before ($t = 0$) and after hydrosilylation (at different times) is shown in Fig. 2 for casting conditions. In all cases, the reaction goes essentially to completion with a residual absorption intensity of the ν(SiH) peak at ~ 2170 cm^{-1} for PL-PMHS close to 0 % (Table 2). As shown in previous studies on hydrosilylation by PMHS for bulkiness allyl precursors [29,30], no SiH groups remained unreacted because the SiH underwent reaction with water (present from air moisture or bound to PC moiety). This led to the hydrolysis of part of the SiH groups into silanol Si–OH groups which may recombine to produce additional SiOSi siloxane crosslinks in the polysiloxane network by Pt-catalyzed dehydrogenative cross-coupling reaction [25,30] of the newly formed silanols with SiH (Scheme 2). Ultimately, new T-crosslinks ($T/SiCH_3O_{3/2}$) are formed into the polysiloxane network. This is confirmed by a significant increase (about 50 %) of the total area of the ν(SiOSi) absorption band (Fig. 1a and b) and by the appearance of ν(SiO) and ν(OH) broad bands (Table 1) in PL-PMHS spectrum indicating the presence of SiOH groups.

3.2.3. Quantitative study of the PL grafting in PMHS films

Since the silane SiH groups may also undergo competitive reactions of hydrolysis, we preferred to measure the graft yield of PL molecule per silicon SiH monomer $z = [PL]/[SiH]_0$ based on intensity of $\nu_{as}(CH_2)$ sharp and strong peak of CH_2 groups where $[SiH]_0$ is the initial total number of SiH groups at $t = 0$ in virgin PMHS for the same sample. With the assumption that the 2:1 (Si:PL) adducts are exclusively formed as explained in Section 3.1.2, (*z)* can also be written as:

$$z = \rho/2 \quad (2)$$

where ρ is the SiH conversion of hydrosylilation yield $\rho = [SiCH]/[SiH]_0$ with an upper boundaries PL-grafting ratio of z_{max} = 50 % for ρ = 100 %. The value of z was calculated using the calibration formula obtained for hydrosilylation in 5% crosslinked PMHS with terminal 1-alkene precursors up to n = 17 in length: $I_{(alkyl\text{-}PMHS,\ 2926)}/I_{(PMHS,\ 2169)} = 0.284\ n \times \rho$ where (n) is the number of methylene group in the grafted hydrocarbon chain $Si(CH_2)_nCH_3$ [30, 31]. In this equation, $I_{(alkyl\text{-}PMHS,\ 2926)}$ and $I_{(PMHS,\ 2169)}$ are the maximum intensities of PL-PMHS for CH_2 at 2926 cm^{-1} and of PMHS (t = 0) for SiH at 2169 cm^{-1}. The results are summarized in Table 2 for n = 17 which was the reference value for estimating the PL graft yield (z) in any experiment by considering the structure of the 2:1 (Si:PL) adduct and the hydrogenation of all remaining double bonds in PL-PMHS films.

The best graft yield (z = 4 %) was obtained by casting and curing at 40 °C for 15 h. All results showed that the hydrosilylation grafting of PL catalyzed by Karstedt's catalyst was achieved in a few dozen minutes in air either at room temperature or slightly above at 40 °C by means of the two methods. Thus, the reaction proceeds under mild conditions in acceptable SiH conversion yield (ρ = 7–8 %). These observations show that PMHS polymer facilitates the hydrosilylation grafting process as compared with reaction of methyl linoleate which was effective only with more reactive chlorohydrosilanes [67, 68].

To summarize, all SiH groups in PMHS films (~ 0.5µm) have reacted under optimized conditions (Residual SiH ~ 0 %) and about 8 % of the SiH group underwent hydrosilylation with C=C double bond. The remainder (~ 90 %) underwent quick reaction with water catalyzed by

Karstedt's catalyst. The formation of Si–O–Si crosslinks hardens the polymer network and increases the film resistance.

3.3. XPS analysis

3.3.1. Characterization of virgin PMHS and functionalized PMHS interfaces

The chemical modification of the PMHS polymer film and the attachment of phospholipid molecule at the interface were confirmed by using XPS spectroscopy (Figures 3–5 and Tables 3–5). The XPS data of pristine PMHS of various crosslinking density ($1 - \alpha$) obtained by increasing the amount of TH crosslinker are in good agreement with the elemental composition of the nominal PHMS structure (Fig. 3a and Table 3), summarized as $(CSiO_{2/2})_{\alpha}(SiO_{3/2})_{(1-\alpha)}$, for fully crosslinked polymer networks predominatly consisting of $D^H/SiHCH_3O_{2/2}$ and $T^H/SiHO_{3/2}$ subunits [16]. In addition, the Si_{2p} high resolution scan spectra of PMHS polymers were resolved in two components with increasing Si-O functionality attributed to D^H and T^H subunits (Fig. 4 and Table 4) in agreement with the Si_{2p} BE values reported for PDMS resins [74]. The fitting results for various D^H/T^H compositions (Table 3) match well the composition determined by quantitative ^{29}Si solid-state nuclear magnetic resonance [16] or FTIR spectroscopy [31] for DH/TH gels prepared in similar conditions. For a more detailed investigation, the C_{1s} high resolution XPS spectra of pristine PMHS ($\alpha = 0.95$) is also shown in Fig. 4. The major C–Si peak at 284.0 eV is assigned to methyl carbons $SiCH_3$ in silicone in agreement with the value of 284.4 eV reported for bulk PDMS polymer [75], along with a small amount of C–C contribution at 284.8 eV attributed to adventitious carbon.

After hydrosilylation of PMHS with PL, peaks attributed respectively to ammonium and phosphate group of the PC unit, nitrogen (N_{1s}, 403 eV) and phosphorus (P_{2s}, 134 eV), appeared

clearly in the XPS spectra (Fig. 3b and Fig. 5). Furthermore, the C_{1s} peak increases dramatically upon grafting of the phospholipid by comparison with pristine PMHS, owing to the presence of the PC groups and the fatty acid ester with a long hydrocarbon chain. For a more detailed investigation, the C_{1s} high resolution XPS spectrum (Fig. 4) can be well fitted by four components at binding energies of 284.0, 284.8, 286.4 and 288.9 eV which were assigned to C–Si, C–C, C–O and C=O, respectively. The C–Si component can be attributed to both $SiCH_3$ carbon of the matrix and $SiCH^{PL}$ carbons in PL-PMHS resulting from hydrosilylation with the internal double bond of phospholipid (CH^{PL} denotes hydrocarbon in SiCH bond formed with PL molecule). Indeed, we expected the C_{1s} binding energy of the Si–C bond in alkyl polysiloxanes [73] to be relatively insensitive to alkyl substitution.

3.3.2. Reaction of water at the PL-PMHS interface

For the grafted more complex surface of PL-PMHS, the shift in the Si_{2p} binding energy to higher value after hydrosilylation (Fig. 4) indicates clearly that essentially oxygen has been incorporated into the material following SiH reaction with H_2O in agreement with FTIR analysis (Section 3.2). Indeed, we expected the BE shift caused by replacement of SiH by $SiCH^{PL}$ to be small in comparison to the shift induced by oxygen [74, 76]. This result was confirmed by Si_{2p} curve-fitting of the high resolution spectrum by two different Si_{2p} environments (Tables 4 and 5). A shown in Fig. 4 for casting treatment, the minor Si_{2p} component $SiO_{2/2}$ is attributed to the $D^{CH}/(CH_3)(CH^{PL})SiO_{2/2}$ silicon units resulting from hydrosilylation reaction (Scheme 1b), and the major $SiO_{3/2}$ component is attributed to $T/SiCH_3O_{3/2}$ new crosslinks units formed by reaction of SiH with H_2O (Scheme 2). The PL-PMHS network is characterized by a ratio D^{CH}/T of about 25/75 (Table 5). To conclude, these observations show a strong increase in the crosslinking

density of the polysiloxane network after hydrosilylation by creation of T-crosslinks in presence of trace of water.

3.3.3. Calculation of PL graft yield at the interface

The XPS results were rationalized by postulating a nominal composition for the PL-PMHS layer made from polysiloxane-bound 2:1 (Si:PL) adducts as sketched in Scheme 1b with additional T-crosslinks (Scheme 2). So we applied the following composition summarized as: $[(C_{44}NO_8P)_{1/2}(CSiO_{2/2})]_{x(1-y)}\ [CSiO_{2/2}]_{(1-x)(1-y)}\ [CSiO_{3/2}]_y$ where the subscript ½ indicates that one PL molecule ($C_{44}NO_8P$) participates in the formation of two Si-CH bonds of D^{CH} unit, x is the fraction of D^{CH} silicon unit bound with phospholipid over the total amount of difunctionnal units including residual D^H, and $y = SiO_{3/2}/100$ is the percentage of $SiO_{3/2}$ (T-crosslinks) as measured by curve-fitting of Si_{2p} spectra (Tables 4 and 5). For simplicity, the T^{CH} content (< 5 %) will be not considered in this calculation because for the Si_{2p} curve-fitting, the expected amounts were not enough to give reliable results. The calculated values are in good agreement with the experimental elemental composition as shown in Table 5 for all experiments.

The PL graft yield (Z) at the interface is defined as a percentage of the surface grafted PL molecule over the total number of silicon atom *[PL]/[Si]* from XPS data. Because of the uncertainty as to the relative weight of phosphorus or nitrogen owing to weak signals, instead of estimating Z as *P/Si* or *N/Si*, we used the experimental ratio *C/Si* of carbon over silicon using the following expression derived from the above stoichiometric structure:

$$Z = (C/Si - 1)/44 \times 100 \qquad (3)$$

This expression is independent of the nature of the Si:PL adduct formed in the polymer network. By assuming the exclusive formation of (2:1) Si:PL adduct, the graft yield can also be written as

$$Z = x(1 - y)/2 = \rho_s/2 \quad (4)$$

with an expression similar to Eq. (2) where ρ_s is the SiH conversion hydrosilylation yield at the surface.

3.3.4. Effect of reaction conditions

3.3.4.1. Casting method

From Fig. 3b and Table 5, the greatest amount of grafted phospholipid ($Z \sim 12\%$) was obtained in condition (1), by casting treatment at 40 °C/15 h. The grafting of hydrophilic PC groups is confirmed by captive air bubble contact angle of $\theta = 0°$ measured on these highly hydrophilic PC-functionalized surfaces (Section 3.4.2). The samples prepared by casting (curing times varying from 1 h to 15 h) are characterized in that the PL graft yield are closed to the upper value limit of $\theta = 0°$. These observations show that the hydrosilylation reaction of internal double bonds of PL molecule has been optimized by thermal activation of hydrosilylation at 40 °C, as expected using Karstedt's catalyst. By comparison of solvent washed layer with the final layer rinsed with water (Table 5), it is shown that washing of the PL-PMHS polymer surface after reaction with solvent (Toluene/$CHCl_3$) was generally sufficient to remove most of the unreacted phospholipid species.

Eq. (4) gives $\rho_s \sim 24$ % for casting condition (1) in Table 5, that is exactly the same value as determined independently by Si_{2p} curve-fitting for $\%SiO_{2/2}$ (24 %). Thus, we found that the residual SiH content D^H (%) is close to 0 % ($1 - x \sim 0$) in good agreement with IR analysis. By considering the formation of polysiloxane-bound 4:1 (Si:PL) adduct, this would give $\rho_s \sim 48$ %

which is clearly in disagreement with the value found for $\%SiO_{2/2}$ (24 %) in this study. To conclude, XPS elemental data and Si_{2p} curves fitting results are consistent by making the assumption that the 2:1 (Si:PL) adducts are preferentially formed. This supports the proposed mechanism of hydrosilylation of internal C=C double bonds of linoleoyl chains of PL molecule, in which only one double bond per chain reacts with SiH (Scheme 1b). The XPS graft yield (*Z)* was about 3 times higher than in the bulk (*z*) as measured by IR absorption (Table 2), showing the preferential reaction of PL at the uppermost layer by the casting method. This method may be useful to those developing thin film gradients for application in material science [79] and surface of biocompatible polymers [80].

3.3.4.2. Immersion method

The surfaces prepared by immersion at 20 °C, conditions (2) and (3) in Table 5, are characterized by lower PL graft yield ($Z \sim 2.5 - 2.7$ %) correlated with a contact angle of 40° higher than for casting method. The values (*z*) and (*Z*) are clearly of same order of magnitude (Table 2 and 5). The results suggest that a homogeneous reaction occurred in the bulk of the film and in the uppermost layer by immersion in swelling solvent. The XPS content of residual hydrophobic SiH group (D^H) at the interface was much higher (25 %) than estimated by casting method (0%). Larger proportions of residual SiH groups are also confirmed by a small negative shift of the $SiO_{2/2}$ component of only 0.1 eV compared with virgin PMHS (Table 4). We believe that SiH groups remained mostly stable after rinsing the samples by immersion in neutral water for 2 h before XPS analysis.

3.4. Surfaces properties

3.4.1. Morphology

The PMHS films were grafted with the phospholipid molecule without any significant physical modification of the surface homogeneity in regard to its wetting and protein resistance ability as shown by AFM microscopy (Fig. 6). Briefly, the pristine PMHS films of thickness about 0.5 μm were flat with AFM roughness (R_q) of 3 nm (Fig. 6a). Homogeneous cured PMHS polymer layers were formed by spin-coating of the sol-gel mixture. Neither crack nor delamination was observed indicating that the layer is bound to the substrate by covalent SiOSi bonds. After hydrosilylation, the uniformity and flatness of initial PMHS were conserved showing the stability of the layer upon reaction and solvent rinsing. Reaction of PL induced always an increase in final roughness at the nanoscale level (R_q) of 13 and 24 nm varying with experimental conditions (Fig. 6b and c). The PL-PMHS film prepared by casting at 40 °C has a roughness higher than by immersing method which can be explained by difference in network reticulation of the PMHS films induced by side reaction with water. AFM (Fig. 6c) and cross-section SEM images (Fig. 7b) also revealed the presence of superficial grooves of less than 100 nm depth showing that there were no grooves descending to the silicon substrate. This peculiarity was not observed for immersion sample as shown in Fig. 6b. Moreover, reaction of PL induced always an increase in final thickness as shown by cross-section SEM images (Fig. 7a and b). This effect has also been observed by ellipsometry in thin PMHS films [62] and for 1-alkene reactions [31].

3.4.2. Wetting properties

The PMHS films show a high hydrophobic behavior, which is related to the quasi absence of residual SiOH in the gel. The static contact angle (θ) with water for the as prepared 5 % crosslinked PMHS was measured after 20 s at 106 ± 1° (Fig. 8a) in ambient condition with an advancing WCA (θ_{adv}) of 108 ± 1° close to the receding WCA (θ_{rec}) of 103 ± 1° (Fig. 8b). The low hysteresis contact angle ($\theta_{adv} - \theta_{rec}$) of 5° for PMHS film is attributed to its low surface

roughness as measured by AFM (Section 3.4.1). According to previous study [16], by changing the DH/TH composition from 95/5 to 50/50, the static WCA decreased by less than about 5° showing that the effect of the various content of Si–H, Si–CH_3 and Si–O is small on the surface energy. After conditioning the interface in pure water for different times, the initial WCA of 5% crosslinked PMHS measured by air captive bubble method (Fig. 8c) was decreased from 105° (after 30 s immersion in water) to 90° (5 minutes) and 47° (24 hours). Thus, the hydrophobic PMHS surface turns into hydrophilic indicating probably that hydrophilic surface SiOH groups are formed upon exposure to neutral water by hydrolysis of some hydrophobic SiH groups.

When the phospholipid surface comes into contact with water, the interfacial morphology may change because of the easy reorientation and migration of phosphoryl groups into the aqueous medium [81,82]. We thus preferred to examine the wetting behavior by the captive air bubble method. By immersing in water the PL-PMHS samples, the WCA was stable after about five minutes (Fig. 8d) indicating a rapid rearrangement of phosphorylcholine groups upon exposure to water. Then, WCAs values did not change after conditioning for 24 h more or several days.

The PL-PMHS surfaces are very hydrophilic suggesting that all substrates tested were grafted with hydrophilic PC in agreement with XPS results (Table 5). In addition, the maximum *N/Si* and *P/Si* ratios and graft yield ($Z \sim 12\%$) determined by XPS are well correlated with the lower WCA measured of about 0° (Fig. 8d) characteristic of a superhydrophilic behavior for PL-PMHS (1) prepared by casting method. In this case, the air bubble could not adhere to the surface and a rolling bubble easily slips away from the surface following slight tilting. For the sample PL-PMHS (2) in Fig. 8d prepared by immersion method ($Z \sim 3\ \%$), the static WCA was increased to 40°, but was nevertheless lower than that of the pristine PMHS (after a few minutes of immersion in water).

3.4.3. Protein adsorption

We previously investigated protein adsorption towards single protein solutions in phosphate saline buffer pH 7.4. The results for bovine serum albumin (BSA) at concentration of 10 µg/ml are reviewed in Table 6 for comparison purpose with casting and immersion XPS data in Table 5. The wettability behavior of the PL-PMHS surfaces was also indicative of a probable protein-repellent character. Interestingly, BSA adsorption results for PL-PMHS are also in good agreement with the present XPS analysis in terms of PL grafting density for samples prepared with the same protocol (immersing or casting). Particularly, the phosphorylcholine modified PL-PMHS samples experienced almost "zero" protein adsorption of 0.05 ng/cm^2 for BSA in the optimized case by casting ($Z \sim 12$ %). By comparison, for samples prepared by immersion ($Z \sim 3$ %), the BSA adsorption is tenfold higher (Table 6). The presence of hydrophobic residual SiH surface groups found by XPS (Table 5) may also play a role in the protein-surface interactions. The low adsorption level on pristine PMHS seems not to be related to the hydrophobic character of the material but probably to hydrolysis of some SiH into hydrophilic SiOH surface groups. Nevertheless, the adsorption of BSA onto PL-PMHS prepared in optimized conditions by casting is 200 times lower than onto PMHS.

4. Conclusion

Polymethylhydrosiloxane films of low roughness and controlled crosslinking density have been prepared and anchored by use of sol-gel chemistry on oxidized silicon wafer by adjusting the molar ratio of methyldiethoxysilane and triethoxysilane reagents. Phosphorylcholine groups were then grafted onto the Si–H functionalized PMHS surface by hydrosilylation of an unsaturated phospholipid molecule bearing linoleoyl chains in the presence of Karstedt's catalyst in air. XPS analysis and water contact angle measurements confirmed the presence of hydrophilic PC groups

on the functionalized PMHS surface. FTIR showed that PL molecule chemically combines with the polysiloxane backbone by covalent silicon–carbon bonds. The reaction leads to the formation of the 2:1 (Si:PL) adduct resultant from one fold addition of SiH group per linoleoyl chain. We showed also that oxygen incorporation into the material had essentially occurred following SiH side reaction with water giving rise to the formation of more highly T-crosslinked polysiloxane film. The efficiency of the hydrosilylation reaction was examined by decreasing the temperature of reaction from 40 °C to 20° C. The correlated wettability changes of surfaces varying from 0° to 40° were determined and explained in terms of interfacial PL grafting density, owing to the partial hydrosilylation of SiH groups. The study shows also a correlation between protein adsorption and the structure of the PC-containing polymers in the case of BSA adsorption. The "grafting to" method we describe is a promising way of obtaining biomaterials permitting to reduce the nonspecific protein adsorption which could be useful in the biomedical field, *e. g*. biosensor, biomaterials, cell culture, substrates for ELISAs methods and biomedical devices.

Acknowledgements

This work was financially supported by FP7 European grant NMP-214538 (BISNES project; Coord. D. Nicolau) and the CNRS. We thank Michel Ramonda (LMCP, UM2) for the AFM pictures, Didier Cot (IEM) for the SEM pictures and Eddy Petit (IEM) for his technical assistance concerning IR spectroscopy. We are also grateful to Philippe Déjardin, Jean-Marc Janot and Emmanuel Troneyl-Perroz for useful discussions about the physicochemical properties and surfaces characterization. The authors thank Damien Quemener for very valuable comments and suggestions on the manuscript.

References

[1] Q. Cao, S. Wu, L. Wang, X. Shi, G. Li, Effects of the morphology of sulfobetaine zwitterionic layers grafted onto a silicone surface on improving the hydrophilic stability, anti-bacterial adhesion properties, and biocompatibility, J. Appl. Polym. Sci. 135 (2018) 46860. https://doi.org/10.1002/app.46860.

[2] Z. Yue, X. Liu, P.J. Molino, G.G. Wallace, Bio-functionalisation of polydimethylsiloxane with hyaluronic acid and hyaluronic acid – Collagen conjugate for neural interfacing, Biomaterials. 32 (2011) 4714–4724. https://doi.org/10.1016/j.biomaterials.2011.03.032.

[3] P. Akkahat, S. Kiatkamjornwong, S. Yusa, V.P. Hoven, Y. Iwasaki, Development of a Novel Antifouling Platform for Biosensing Probe Immobilization from Methacryloyloxyethyl Phosphorylcholine-Containing Copolymer Brushes, Langmuir. 28 (2012) 5872–5881. https://doi.org/10.1021/la204229t.

[4] M. Tanaka, K. Yoshioka, Y. Hirata, M. Fujimaki, M. Kuwahara, O. Niwa, Design and Fabrication of Biosensing Interface for Waveguide-Mode Sensor, Langmuir. 29 (2013) 13111–13120. https://doi.org/10.1021/la402802u.

[5] T. Goda, K. Ishihara, Soft contact lens biomaterials from bioinspired phospholipid polymers, Expert Rev. Med. Devices. 3 (2006) 167–174. https://doi.org/10.1586/17434440.3.2.167.

[6] Y. Xu, M. Takai, K. Ishihara, Phospholipid Polymer Biointerfaces for Lab-on-a-Chip Devices, Ann. Biomed. Eng. 38 (2010) 1938–1953. https://doi.org/10.1007/s10439-010-0025-3

[7] Y. Kumada, S. Katoh, H. Imanaka, K. Imamura, K. Nakanishi, Development of a one-step ELISA method using an affinity peptide tag specific to a hydrophilic polystyrene surface, J. Biotechnol. 127 (2007) 288–299. https://doi.org/10.1016/j.jbiotec.2006.07.011.

[8] X. Liu, L. Yuan, D. Li, Z. Tang, Y. Wang, G. Chen, H. Chen, J.L. Brash, Blood compatible materials: state of the art, J. Mater. Chem. B. 2 (2014) 5718–5738. https://doi.org/10.1039/C4TB00881B.

[9] Z. Zhang, M. Zhang, S. Chen, T.A. Horbett, B.D. Ratner, S. Jiang, Blood compatibility of surfaces with superlow protein adsorption, Biomaterials. 29 (2008) 4285–4291. https://doi.org/10.1016/j.biomaterials.2008.07.039.

[10] Q. Li, J. Imbrogno, G. Belfort, X.-L. Wang, Making polymeric membranes antifouling via “grafting from” polymerization of zwitterions, J. Applied Polym. Sci. 132 (2015). https://doi.org/10.1002/app.41781.

[11] H.-C. Yang, J. Luo, Y. Lv, P. Shen, Z.-K. Xu, Surface engineering of polymer membranes via mussel-inspired chemistry, J. Membr. Sci. 483 (2015) 42–59. https://doi.org/10.1016/j.memsci.2015.02.027.

[12] H. Murata, B.-J. Chang, O. Prucker, M. Dahm, J. Rühe, Polymeric coatings for biomedical devices, Surf. Sci. 570 (2004) 111–118. https://doi.org/10.1016/j.susc.2004.06.185.

[13] I. Luzinov, S. Minko, V.V. Tsukruk, Adaptive and responsive surfaces through controlled reorganization of interfacial polymer layers, Prog. Polym. Sci. 29 (2004) 635–698.

[14] L. Zhai, Stimuli-responsive polymer films, Chem. Soc. Rev. 42 (2013) 7148–7160. https://doi.org/10.1039/C3CS60023H.

[15] E.P. Pluedemann, Silane Coupling Agents, Plenum Press, New York, 1982.

[16] T. Thami, B. Bresson, C. Fretigny, Tailoring of elastomeric grafted coating via sol-gel chemistry of crosslinked polymethylhydrosiloxane, J. Appl. Polym. Sci. 104 (2007) 1504–1516. https://doi.org/10.1002/pola.22691.
[17] M.A. Brook, Silicon, in Organic, Organometallic and Polymer Chemistry, John Wiley, New York, 1995.
[18] A. Saxena, M. Markanday, A. Sarkar, V.K. Yadav, A.S. Brar, A Systematic Approach To Decipher the Microstructure of Methyl Hydrosiloxane Copolymers and Its Impact on Their Reactivity Trends, Macromolecules. 44 (2011) 6480–6487. https://doi.org/10.1021/ma201195c.
[19] J.L. Speier, Homogeneous Catalysis of Hydrosilation by Transition Metals, Adv. Organomet. Chem. 17 (1979) 407–447. https://doi.org/10.1016/S0065-3055(08)60328-7
[20] L.N. Lewis, Chemical Catalysis by Colloids and Clusters, Chem. Rev. 93 (1993) 2693–2730. https://doi.org/10.1021/cr00024a006.
[21] A.K. Roy, A review of recent progress in catalyzed homogeneous hydrosilation (Hydrosilylation), in: R. West, Hill A. F, Fink M. J (Eds.), Ad. Organomet. Chem., 2008: pp. 1–59. https://doi.org/10.1016/S0065-3055(07)55001-X.
[22] E.Y. Lukevics, Latest Research on the Hydrosilylation Reaction, Russ. Chem. Rev. 46 (1977) 264–277. https://doi.org/10.1070/RC1977v046n03ABEH002131.
[23] B. Marciniec, Comprehensive Handbook on Hydrosilylation, Pergamon, New York, 1992.
[24] S. Putzien, O. Nuyken, F.E. Kuehn, Functionalized polysilalkylene siloxanes (polycarbosiloxanes) by hydrosilylation-Catalysis and synthesis, Prog. Polym. Sci. 35 (2010) 687–713. https://doi.org/10.1016/j.progpolymsci.2010.01.007.
[25] Y. Satoh, M. Igarashi, K. Sato, S. Shimada, Highly Selective Synthesis of Hydrosiloxanes by Au-Catalyzed Dehydrogenative Cross-Coupling Reaction of Silanols with Hydrosilanes, ACS Catal. 7 (2017) 1836–1840. https://doi.org/10.1021/acscatal.6b03560.
[26] E. Lukevics, Z.V. Belyakova, M.G. Pomerantseva, M.G. Voronkov, Hydrosilylation. Recent Achievments, J. Organomet. Chem. Libr. 5 (1977) 1–179.
[27] A. El Kadib, N. Katir, N. Marcotte, K. Molvinger, A. Castel, P. Riviere, D. Brunel, Nanocomposites from natural templates based on fatty compound-functionalised siloxanes, J. Mater. Chem. 19 (2009) 6004–6014. https://doi.org/10.1039/b906448f.
[28] O. Mukbaniani, G. Titvinidze, T. Tatrishvili, N. Mukbaniani, W. Brostow, D. Pietkiewicz, Formation of polymethylsiloxanes with alkyl side groups, J. Appl. Polym. Sci. 104 (2007) 1176–1183. https://doi.org/10.1002/app.25734.
[29] K. Amro, S. Clement, P. Dejardin, W.E. Douglas, P. Gerbier, J.-M. Janot, T. Thami, Supported thin flexible polymethylhydrosiloxane permeable films functionalised with silole groups: new approach for detection of nitroaromatics, J. Mater. Chem. 20 (2010) 7100–7103. https://doi.org/10.1039/c0jm01165g.
[30] G. Nasr, H. Bestal, M. Barboiu, B. Bresson, T. Thami, Functionalization of Polymethylhydrosiloxane Gels with an Allyl Ureido Benzocrown Ether Derivative: Complexation Properties, J. Appl. Polym. Sci. 111 (2009) 2785–2797. https://doi.org/10.1002/app.29327.
[31] T. Thami, G. Nasr, H. Bestal, A. Van der Lee, B. Bresson, Fonctionalization of Surface-Grafted Polymethylhydrosiloxane with Alkyl Side Chains, J. Polym. Sci. Part A: Polym. Chem. 46 (2008) 3546–3562. https://doi.org/10.1002/pola.22691.

[32] H. Chen, L. Yuan, W. Song, Z. Wu, D. Li, Biocompatible polymer materials: Role of protein-surface interactions, Prog. Polym. Sci. 33 (2008) 1059–1087. https://doi.org/10.1016/j.progpolymsci.2008.07.006.
[33] I. Liascukiene, K. El Kirat, M. Beauvais, S.J. Asadauskas, J.-F. Lambert, J. Landoulsi, Lipid Layers on Nanoscale Surface Topography: Stability and Effect on Protein Adsorption, Langmuir. 33 (2017) 4414–4425. https://doi.org/10.1021/acs.langmuir.7b00431.
[34] O. Albrecht, D.S. Johnston, C. Villaverde, D. Chapman, Stable biomembrane surfaces formed by phospholipid polymers, Biochim. Biophys. Acta. 687 (1982) 165–169. https://doi.org/10.1016/0005-2736(82)90542-9.
[35] D.S. Johnston, S. Sanghera, M. Pons, D. Chapman, Phospholipid polymers - synthesis and spectral characteristics, Biochim. Biophys. Acta. 602 (1980) 57–69. https://doi.org/10.1016/0005-2736(80)90289-8.
[36] A.L. Lewis, Phosphorylcholine-based polymers and their use in the prevention of biofouling, Colloids Surf. B. 18 (2000) 261–275. https://doi.org/10.1016/s0927-7765(99)00152-6.
[37] T. Nakaya, Y.J. Li, Recent progress of phospholipid polymers, Des. Monomers Polym. 6 (2003) 309–351. https://doi.org/10.1163/156855503771816813.
[38] G. Kim, S. Park, J. Jung, K. Heo, J. Yoon, H. Kim, I.J. Kim, J.R. Kim, J.I. Lee, M. Ree, Novel Brush Polymers with Phosphorylcholine Bristle Ends: Synthesis, Structure, Properties, and Biocompatibility, Adv. Funct. Mater. 19 (2009) 1631–1644. https://doi.org/10.1002/adfm.200801680.
[39] W. Feng, S.P. Zhu, K. Ishihara, J.L. Brash, Adsorption of fibrinogen and lysozyme on silicon grafted with poly(2-methacryloyloxyethyl phosphorylcholine) via surface-initiated atom transfer radical polymerization, Langmuir. 21 (2005) 5980–5987. https://doi.org/10.1021/la050277i.
[40] M. Kobayashi, Y. Terayama, N. Hosaka, M. Kaido, A. Suzuki, N. Yamada, N. Torikai, K. Ishihara, A. Takahara, Friction behavior of high-density poly(2-methacryloyloxyethyl phosphorylcholine) brush in aqueous media, Soft Matter. 3 (2007) 740–746. https://doi.org/10.1039/b615780g.
[41] M. Kyomoto, T. Moro, Y. Takatori, H. Kawaguchi, K. Nakamura, K. Ishihara, Self-initiated surface grafting with poly(2-methacryloyloxyethyl phosphorylcholine) on poly(ether-ether-ketone), Biomaterials. 31 (2010) 1017–1024. https://doi.org/10.1016/j.biomaterials.2009.10.055.
[42] M. Kyomoto, K. Ishihara, Self-Initiated Surface Graft Polymerization of 2-Methacryloyloxyethyl Phosphorylcholine on Poly(ether ether ketone) by Photoirradiation, ACS Appl. Mater. Interfaces. 1 (2009) 537–542. https://doi.org/10.1021/am800260t.
[43] T. Hoshi, R. Matsuno, T. Sawaguchi, T. Konno, M. Takai, K. Ishihara, Protein adsorption resistant surface on polymer composite based on 2D-and 3D-controlled grafting of phospholipid moieties, Appl. Surf. Sci. 255 (2008) 379–383. https://doi.org/10.1016/j.apsusc.2008.06.145.
[44] N. Morimoto, A. Watanabe, Y. Iwasaki, K. Akiyoshi, K. Ishihara, Nano-scale surface modification of a segmented polyurethane with a phospholipid polymer, Biomaterials. 25 (2004) 5353–5361. https://doi.org/10.1016/j.biomaterials.2003.12.047.
[45] L. Yan, K. Ishihara, Graft copolymerization of 2-methacryloyloxyethyl phosphorylcholine to cellulose in homogeneous media using atom transfer radical polymerization for

providing mew hemocompatible coating materials, J. Polym. Sci., Part A: Polym. Chem. 46 (2008) 3306–3313. https://doi.org/10.1002/pola.22670.
[46] T. Goda, T. Konno, M. Takai, T. Moro, K. Ishihara, Biomimetic phosphorylcholine polymer grafting from polydimethylsiloxane surface using photo-induced polymerization, Biomaterials. 27 (2006) 5151–5160. https://doi.org/10.1016/j.biomaterials.2006.05.046.
[47] J.-H. Seo, R. Matsuno, T. Konno, M. Takai, K. Ishihara, Surface tethering of phosphorylcholine groups onto poly(dimethylsiloxane) through swelling-deswelling methods with phospholipids moiety containing ABA-type block copolymers, Biomaterials. 29 (2008) 1367–1376. https://doi.org/10.1016/j.biomaterials.2007.11.039.
[48] K. Ishihara, B. Ando, M. Takai, Phosphorylcholine Group-immobilized Surface Prepared on Polydimethylsiloxane Membrane by In Situ Reaction for Its Reduced Biofouling, Nanobiotechnology. 3 (2007) 83–88. https://doi.org/10.1007/s12030-008-9006-0.
[49] R.E. Holmlin, X.X. Chen, R.G. Chapman, S. Takayama, G.M. Whitesides, Zwitterionic SAMs that resist nonspecific adsorption of protein from aqueous buffer, Langmuir. 17 (2001) 2841–2850. https://doi.org/10.1021/la0015258.
[50] V.A. Tegoulia, W.S. Rao, A.T. Kalambur, J.R. Rabolt, S.L. Cooper, Surface properties, fibrinogen adsorption, and cellular interactions of a novel phosphorylcholine-containing self-assembled monolayer on gold, Langmuir. 17 (2001) 4396–4404. https://doi.org/10.1021/la001790t.
[51] S.F. Chen, J. Zheng, L.Y. Li, S.Y. Jiang, Strong resistance of phosphorylcholine self-assembled monolayers to protein adsorption: Insights into nonfouling properties of zwitterionic materials, J. Am. Chem. Soc. 127 (2005) 14473–14478. https://doi.org/10.1021/ja054169u.
[52] Y.C. Chung, Y.H. Chiu, Y.W. Wu, Y.T. Tao, Self-assembled biomimetic monolayers using phospholipid-containing disulfides, Biomaterials. 26 (2005) 2313–2324. https://doi.org/10.1016/j.biomaterials.2004.06.043.
[53] A.S. Kohler, P.J. Parks, D.L. Mooradian, G.H.R. Rao, L.T. Furcht, Platelet adhesion to novel phospholipid materials: Modified phosphatidylcholine covalently immobilized to silica, polypropylene, and PTFE materials, J. Biomed. Mater. Res. 32 (1996) 237–242. https://doi.org/10.1002/(sici)1097-4636(199610)32:2<237::aid-jbm13>3.0.co;2-g.
[54] J.R. Lu, E.F. Murphy, T.J. Su, A.L. Lewis, P.W. Stratford, S.K. Satija, Reduced protein adsorption on the surface of a chemically grafted phospholipid monolayer, Langmuir. 17 (2001) 3382–3389. https://doi.org/10.1021/la0017429.
[55] A.A. Durrani, J.A. Hayward, D. Chapman, Biomembranes as models for polymer surfaces. 2. The syntheses of reactive species for covalent coupling of phosphorylcholine to polymer surfaces, Biomaterials. 7 (1986) 121–125. https://doi.org/10.1016/0142-9612(86)90068-2.
[56] J.A. Hayward, A.A. Durrani, C.J. Shelton, D.C. Lee, D. Chapman, Biomembranes as models for polymer surfaces. 3. Characterization of a phosphorylcholine surface covalently bound to glass, Biomaterials. 7 (1986) 126–131. https://doi.org/10.1016/0142-9612(86)90069-4.
[57] S.-H. Ye, C.A. Johnson, J.R. Woolley, H. Murata, L.J. Gamble, K. Ishihara, W.R. Wagner, Simple surface modification of a titanium alloy with silanated zwitterionic phosphorylcholine or sulfobetaine modifiers to reduce thrombogenicity, Colloids Surf. B. 79 (2010) 357–364. https://doi.org/10.1016/j.colsurfb.2010.04.018.

[58] A.L. Lewis, Z.L. Cumming, H.H. Goreish, L.C. Kirkwood, L.A. Tolhurst, P.W. Stratford, Crosslinkable coatings from phosphorylcholine-based polymers, Biomaterials. 22 (2001) 99–111. https://doi.org/10.1016/s0142-9612(00)00083-1.
[59] L. Děkanovský, R. Elashnikov, M. Kubiková, B. Vokatá, V. Švorčík, O. Lyutakov, Dual-Action Flexible Antimicrobial Material: Switchable Self-Cleaning, Antifouling, and Smart Drug Release, Adv. Funct. Mater. 29 (2019) 1901880. https://doi.org/10.1002/adfm.201901880.
[60] O. Guselnikova, R. Elashnikov, P. Postnikov, V. Svorcik, O. Lyutakov, Smart, Piezo-Responsive Polyvinylidenefluoride/Polymethylmethacrylate Surface with Triggerable Water/Oil Wettability and Adhesion, ACS Appl. Mater. Interfaces. 10 (2018) 37461–37469. https://doi.org/10.1021/acsami.8b06840.
[61] L. Ferez, T. Thami, E. Akpalo, V. Flaud, L. Tauk, J.-M. Janot, P. Dejardin, Interface of Covalently Bonded Phospholipids with a Phosphorylicholine Head: Characterization, Protein Nonadsorption, and Further Functionalization, Langmuir. 27 (2011) 11536–11544. https://doi.org/10.1021/la202793k.
[62] L. Tauk, T. Thami, L. Ferez, A. Kocer, J.-M. Janot, P. Dejardin, Thin phosphatidylcholine films as background surfaces with further possibilities of functionalization for biomedical applications, Colloids Surf. B. 101 (2013) 189–195. https://doi.org/10.1016/j.colsurfb.2012.06.028.
[63] F. Delpech, S. Asgatay, A. Castel, P. Riviere, M. Riviere-Baudet, A. Amin-Alami, J. Manriquez, Toward new biosilicones: hydrosilylation of fish oil unsaturated fatty acid esters, Appl. Organomet. Chem. 15 (2001) 626–634. https://doi.org/10.1002/aoc.198.
[64] G. Lligadas, L. Callau, J.C. Ronda, M. Galia, V. Cadiz, Novel organic-inorganic hybrid materials from renewable resources: Hydrosilylation of fatty acid derivatives, J. Polym. Sci. Part A: Polym. Chem. 43 (2005) 6295–6307. https://doi.org/10.1002/pola.21039.
[65] N. Saghian, D. Gertner, Hydrosilylation of long chain unsaturated fatty acid esters, J. Am. Oil Chem. Soc. 51 (1974) 363–367. https://doi.org/10.1007/BF02632385.
[66] A. Behr, A. Westfechtel, J.P. Gomes, Catalytic processes for the technical use of natural fats and oils, Chem. Eng. Technol. 31 (2008) 700–714. https://doi.org/10.1002/ceat.200800035.
[67] A. Behr, F. Naendrup, D. Obst, The synthesis of silicon oleochemicals by hydrosilylation of unsaturated fatty acid derivatives, Eur. J. Lipid Sci. Tech. 104 (2002) 161–166. https://doi.org/10.1002/1438-9312(200203)104:3<161::aid-ejlt161>3.0.co;2-n.
[68] A. Behr, F. Naendrup, D. Obst, Platinum-catalysed hydrosilylation of unsaturated fatty acid esters, Adv. Synth. Catal. 344 (2002) 1142–1145. https://doi.org/10.1002/1615-4169(200212)344:10<1142::aid-adsc1142>3.0.co;2-p.
[69] A. El Kadib, N. Katir, A. Castel, F. Delpech, P. Riviere, Hydrosilylation of unsaturated fatty acid N-phenyl amides, Appl. Organomet. Chem. 21 (2007) 590–594. https://doi.org/10.1002/aoc.1240.
[70] A. El Kadib, A. Castel, F. Delpech, P. Rivière, Silylation of triacylglycerol: an easy route to new biosiloxanes, Chem. Phys. Lipids. 148 (2007) 112–120. https://doi.org/10.1016/j.chemphyslip.2007.05.002.
[71] W. Yang, S. Chen, G. Cheng, H. Vaisocherová, H. Xue, W. Li, J. Zhang, S. Jiang, Film Thickness Dependence of Protein Adsorption from Blood Serum and Plasma onto Poly(sulfobetaine)-Grafted Surfaces, Langmuir. 24 (2008) 9211–9214. https://doi.org/10.1021/la801487f.

[72] Z. Zhang, S. Chen, S. Jiang, Dual-Functional Biomimetic Materials: Nonfouling Poly(carboxybetaine) with Active Functional Groups for Protein Immobilization, Biomacromolecules. 7 (2006) 3311–3315. https://doi.org/10.1021/bm060750m.
[73] J.H. Scofield, Hartree-Slater subshell photoionization cross-sections at 1254 and 1487eV, J. Electron Spectrosc. Relat. Phenom. 8 (1976) 129–137. https://doi.org/10.1016/0368-2048(76)80015-1.
[74] L.A. O'Hare, B. Parbhoo, S.R. Leadley, Development of a methodology for XPS curve-fitting of the Si 2p core level of siloxane materials, Surf. Interface Anal. 36 (2004) 1427–1434. https://doi.org/10.1002/sia.1917.
[75] G. Beamson, D. Briggs, High resolution XPS of Organic Polymers, Wiley, Chichester, 1992.
[76] M.R. Alexander, R.D. Short, F.R. Jones, W. Michaeli, C.J. Blomfield, A study of HMDSO/O2 plasma deposits using a high-sensitivity and -energy resolution XPS instrument: curve fitting of the Si 2p core level, Appl. Surf. Sci. 137 (1999) 179–183. https://doi.org/10.1016/s0169-4332(98)00479-6.
[77] C. Maldonado-Codina, P.B. Morgan, In vitro water wettability of silicone hydrogel contact lenses determined using the sessile drop and captive bubble techniques, J Biomed. Mater. Res. A. 83A (2007) 496–502. https://doi.org/10.1002/jbm.a.31260.
[78] A.L. Smith, Chemical Analysis, Vol. 112: The Analytical Chemistry of Silicones, Wiley, New York, 1991.
[79] C. Cui, A. Kirkeminde, B. Kannan, M.M. Collinson, D.A. Higgins, Spatiotemporal Evolution of Fixed and Mobile Dopant Populations in Silica Thin-Film Gradients as Revealed by Single Molecule Tracking, J. Phys. Chem. C. 115 (2011) 728–735. https://doi.org/10.1021/jp109757k.
[80] J.C. Meredith, A.P. Smith, A. Karim, E.J. Amis, Combinatorial materials science for Polymer Thin-Film Dewetting, Macromolecules. 33 (2000) 9747–9756. https://doi.org/10.1021/ma001298g.
[81] K. Futamura, R. Matsuno, T. Konno, M. Takai, K. Ishihara, Rapid development of hydrophilicity and protein adsorption resistance by polymer surfaces bearing phosphorylcholine and naphthalene groups, Langmuir. 24 (2008) 10340–10344. https://doi.org/10.1021/la801017h.
[82] S. Yang, S.-P. Zhang, F.M. Winnik, F. Mwale, Y.-K. Gong, Group reorientation and migration of amphiphilic polymer bearing phosphorylcholine functionalities on surface of cellular membrane mimicking coating, J. Biomed. Mater. Res-A. 84A (2008) 837–841. https://doi.org/10.1002/jbm.a.31418.

Figure and Table captions

Scheme 1. (a) Synthesis of crosslinked polymethylhydrosiloxane (PMHS) films onto silicon wafer. (b) Surface hydrosilylation grafting of a PMHS films with phospholipid molecule (PL).

Scheme 2. Reaction of PMHS with H_2O: Hydrolysis of hydrosiloxane Si–H bonds of PMHS monomer (–OSi(H)CH_3–) to silanols (–OSi(OH)CH_3–) and dehydrogenative cross-coupling reaction of silanols with SiH groups of PMHS monomer catalyzed by Karstedt's catalyst in presence of air.

Figure 1. (top) IR spectra of same PMHS sample before and after PL hydrosilylation by casting method: (a) virgin 5 % crosslinked PMHS thin film (0.64 μm), and (b) functionalized PL-PMHS. (bottom) IR spectrum (c) of the starting PL molecule.

Figure 2. IR spectra of different PMHS samples (same thickness of 0.50 μm at t = 0) after stopping the hydrosilylation with PL at various times by washing and drying procedure (conditions: casting, 40°C, 1.5-fold excess of phospholipid over SiH, 4.2 mol % Karstedt catalyst over SiH, solvent: toluene).

Figure 3. XPS survey spectra of the surfaces of: (a) pristine PMHS of different crosslinking density (α) (0.95, 0.85 and 0.70) and (b) PMHS ($\alpha = 0.95$) treated with phospholipid (PL-PMHS) (1) by casting at 40 °C for 15 h and (2) by immersing at 20 °C for 6 h. The corresponding surface elemental compositions (C, Si, O, N, P) are summarized in Tables 3 and 5.

Figure 4. High resolution C_{1s} and Si_{2p} XPS spectra and curves fit (solid line) of: (top) pristine PMHS (crosslinking density $\alpha = 0.95$), (bottom) PMHS treated with phospholipid (PL-PMHS) by casting and curing at 40 °C. (dashed line) Secondary peaks $Si_{2p}^{1/2}$.

Figure 5. High resolution N_{1s} and P_{2p} XPS spectra of PL-PMHS after hydrosylilation by casting and curing at 40 °C.

Figure 6. Representative AFM images of PMHS before and after modification: (a) pristine PMHS film, (b) PL-PMHS prepared by immersion and (c) PL-PMHS prepared by casting.

Figure 7. Cross-section SEM images of (a) pristine PMHS and (b) PL-PMHS prepared by casting.

Figure 8. Contact angles of PMHS surfaces (crosslinking density $\alpha = 0.95$): (a) static WCA (θ) measured by the sessile drop method in air, (b) advancing (θ_{adv}) and receding (θ_{rec}) WCAs by increasing/decreasing drop volume method, and static WCA (θ) measured by captive air bubble method at different conditioning times of the interface in water for (c) pristine PMHS and (d) PL-PMHS after surface modification (1) by casting at 40 °C for 15 h and (2) by immersing at 20° C for 6 h.

Table 1. Infrared peak assignments of silicon wafer thin films grafted with PMHS (5% crosslinked), functionalized with PL molecule (PL-PMHS), and pure PL molecule (wafer).

Table 2. Hydrosilylation of 5 % crosslinked PMHS thin films (~ 0.5 µm) with 1,2-dilinoleoyl-sn-glycero-3-phosphorylcholine (18:2 Cis) (PL) (1.5-fold excess of phospholipid over SiH, 4.2 and 1.2 mol % Karstedt catalyst over SiH in exp. (1, 2) and (3, 4) respectively, solvent: toluene).

Table 3. XPS analysis summarizing at the surface of various crosslinked PMHS thin films (~ 0.5 µm) prepared on silicon by sol-gel curing of methyldiethoxylsilane (DH) / triethoxylane (TH) mixtures.

Table 4. Binding energies determined by curve-fitting of the Si_{2p} XPS high resolution spectra in two components, $SiO_{2/2}$ (D^H, D^{CH}) and $SiO_{3/2}$ (T^H, T, T^{CH}), indicating the structure of the various possible siloxane subunits encountered in as prepared crosslinked PMHS of various degree of crosslinking and in PL-PMHS derived from 5 % crosslinked PMHS after different treatments.

Table 5. XPS analysis summarizing changes in elemental composition and SiO contents at the surface of phospholipid grafted PL-PMHS prepared in different reaction conditions by hydrosilylation grafting of 5 % crosslinked PMHS thin films (~ 0.5 µm) with 1,2-dilinoleoyl-sn-glycero-3-phosphorylcholine (18:2 Cis) (PL) and corresponding captive air bubble WCA (θ).

Table 6. Bovine serum albumin (BSA) adsorption on PL functionalized and virgin PMHS films [61,62].

Table 1

Group frequency	Band position (cm^{-1})		
	PMHS	PL-PMHS	PL
ν(OH)		3380[a]	3320[a]
$\nu(CH)_{alkene}$		n. d.	3009
$\nu_{as}(CH_3)$	2967	2960	2956
$\nu_{as}(CH_2)$		2926	2926
$\nu_{s}(CH_2)$		2856	2854
ν(Si–H)	2169	~ 2170[b]	
ν(C=O)		1736	1737
$\nu(C=C)_{alkene}$		n. d.	1652
$\delta(CH_2)$		~ 1470[c]	1466
$\delta_{as}(SiCH_3)$	1410	1411	
$\delta_{s}(SiCH)$		1271	
$\delta_{s}(SiCH_3)$	1262	1260 sh	
ν(P=O)		~ 1250 sh	1244
$\nu_{as}(SiOSi))$	1094, 1055 sh	1045	
ν(PO)		~ 1090 sh	1091
$\nu(SiO)_{SiOH}$		~ 920	
δ(SiH) (scissoring)	890, 838	~ 836[b]	
$\delta(CH)_{alkene}$		n. d.	725[d]

sh, shoulder; ν, stretching mode; as, asymmetric; s, symmetric; δ, bending mode; n. d., not detected.

[a] Very broad band.

[b] Residual peak.

[c] Broad envelop.

[d] Out-of-plane CH bend attributed to of 1,2 disubtituted cis-alkene.

Table 2

Exp.	Conditions	$[PL]_0$ (mM)[a]	Time (h)	Graft yield z (%)[b]	Residual SiH (%)
1	Casting 40 °C	26	1	3.5 ± 0.5	~ 0
2	Casting 40 °C	26	15	4.0 ± 0.5	~ 0
3	Immersion 22 °C	3.2	1	2.9 ± 0.5	~ 0
4	Immersion 22 °C	3.2	6	3.5 ± 0.5	~ 0

[a] Concentration of phospholipid at $t = 0$ in toluene.

[b] Based on IR absorption (± SD over three samples); SiH conversion of hydrosilylation can be calculated by $\rho = 2z$ for 2:1 (Si:PL) adduct.

Table 3

Crosslinked PMHS	Element (atom %)					Si(2p) (%)	
	C	Si	O	O/Si	C/Si	$SiO_{2/2}$	$SiO_{3/2}$
Theoretical bulk composition (1)[a]	31.9	33.6	34.5	1.03	0.95	95	5
As prepared, $\alpha = 0.95$ (1)	30.2	37.8	32.0	0.85	0.80	90	10
Theoretical bulk composition (2)[a]	29.1	34.2	36.7	1.07	0.85	85	15
As prepared, $\alpha = 0.85$ (2)	26.7	37.9	35.4	0.93	0.70	83	17
Theoretical bulk composition (3)[a]	24.6	35.1	40.3	1.15	0.70	70	30
As prepared, $\alpha = 0.70$ (3)[b]	22.4	37.4	40.2	1.07	0.60	73	27

[a] Calculated on the theoretical bulk composition D^H/T^H summarized as: $(CSiO_{2/2})_{\alpha}(SiO_{3/2})_{1-\alpha}$ where $\alpha/1-\alpha$ is the ratio of DH/TH mixture (mol %).

[b] The presence of trace of fluor (< 0.5 %) at the interface (Fig. 3a) was neglected in the calculation of atomic %.

Table 4

Material	Treatment	Siloxane units[a]	Binding energy (eV) for Si $2p^{3/2}$ doublet
Crosslinked PMHS[b]	As prepared	D^H	101.5 ± 0.1
		T^H	102.4 ± 0.1
Grafted PL-PMHS	Casting 40 °C, 15h	D^{CH}	101.2 ± 0.1
		T (major) + T^{CH}	102.1 ± 0.1
Grafted PL-PMHS	Immersing 22 °C, 1h/6h	D^{CH} + D^H	101.4 ± 0.1
		T (major) + T^{CH}	102.1 ± 0.1

[a] Standard abbreviations for D^H, T^H and D, T are used, it also includes D^{CH} /$(CH_3)(CH^{PL})SiO_{2/2}$ and T^{CH} /$(CH^{PL})SiO_{3/2}$. PDMS resins [74]: D 102.0 eV; T 102.7 eV.

[b] Binding energies for 5, 15 and 30 % (mol %) TH-crosslinked PMHS are of same values (± 0.1 eV).

Table 5

Condition	Element (atom %)[a]					Si(2p) (%)		Residual D^H (%)[b]	Graft yield Z (%)[c]	θ (°)[d]
	C	Si	O	N	P	$SiO_{2/2}$	$SiO_{3/2}$			
Theoretical bulk composition (1)[b]	63.8	10.1	23.7	1.2	1.2	24	76	0	12	
Casting 40 °C/15h, solvent washed (1)	63.6	7.3	25.9	1.4	1.8					
(1) + water washed, 2 h	60.0	9.6	27.6	1.2	1.6	24[e]	76	0	12	0
Theoretical bulk composition (2)[b]	45.0	21.2	32.8	0.5	0.5	31	69	26	2.5	
Immersing 22 °C, 1h (2)	46.1	21.7	31.2	0.6	0.4	31	69	26	2.5	40
Theoretical bulk composition (3)[b]	45.5	20.7	32.6	0.6	0.6	28	72	23	2.7	
Immersing 22 °C, 6 h (3)	46.8	21.3	30.9	0.5	0.5	28	72	23	2.7	40

[a] The presence of trace of platinum (< 0.15 %) at the interfaces (Fig. 3b) was neglected in the calculation of atomic %.

[b] Calculated (Section 3.3.3).

[c] Calculated from Eq. (3). SiH conversion yield of hydrosilylation at the surface can be calculated by $\rho_s = 2Z$ for 2:1 (Si:PL) adduct.

[d] At least three samples were measured. Data precision is about ± 2.5° (Fig. 8d).

[e] SD ± 1 % for three samples.

Table 6

Film	Conditions	Adsorbed BSA protein (ng/cm^2)[a]
Virgin PMHS [62]		10 ± 2
PL functionalized PMHS [61]	Casting 15 h	0.05 ± 0.04
PL functionalized PMHS [62]	Immersion 6 h	0.5 ± 0.3

[a] BSA concentration 10 µg/mL. All samples measured after conditioning overnight in phosphate saline buffer 10 mM (NaCl 150 mM) at pH 7.4.

Scheme 1

Click here to download high resolution image

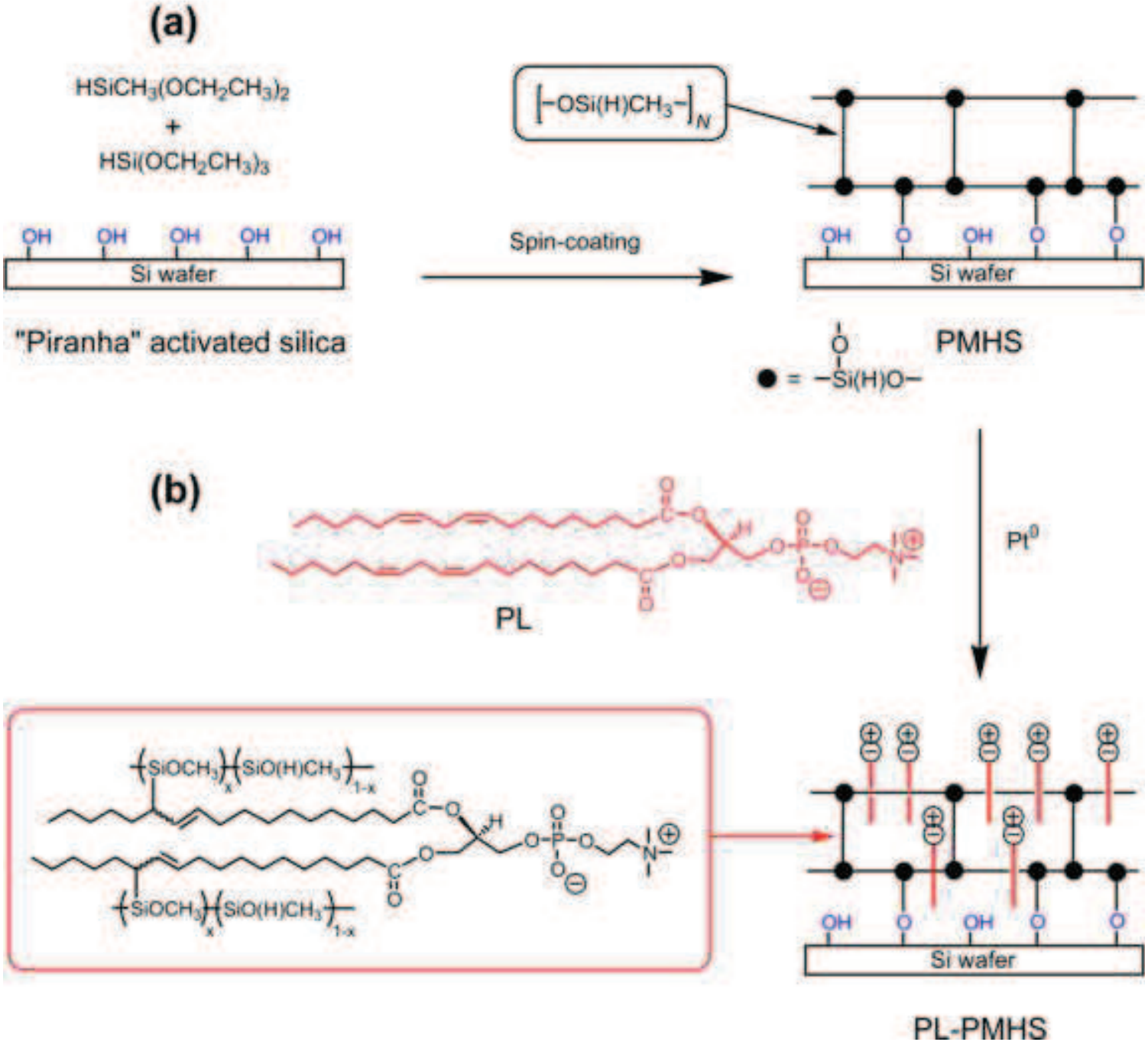

Scheme 2

Click here to download high resolution image

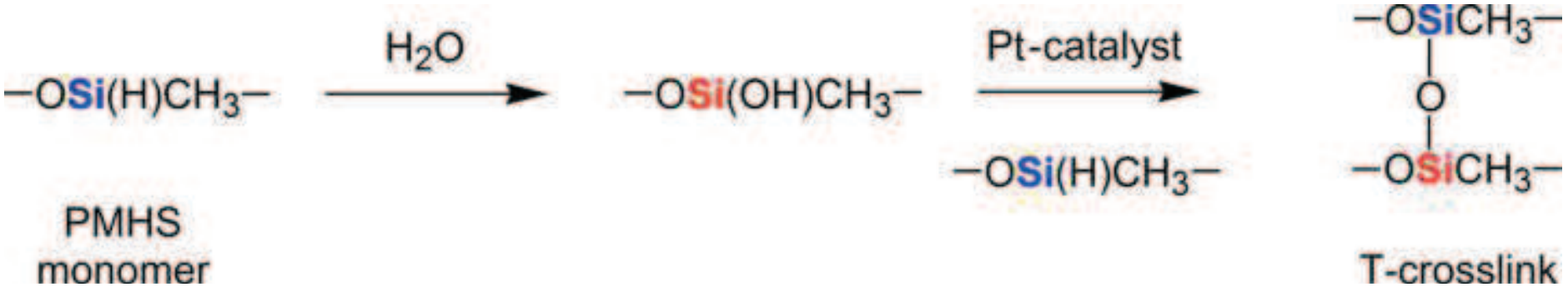

Fig. 1
Click here to download high resolution image

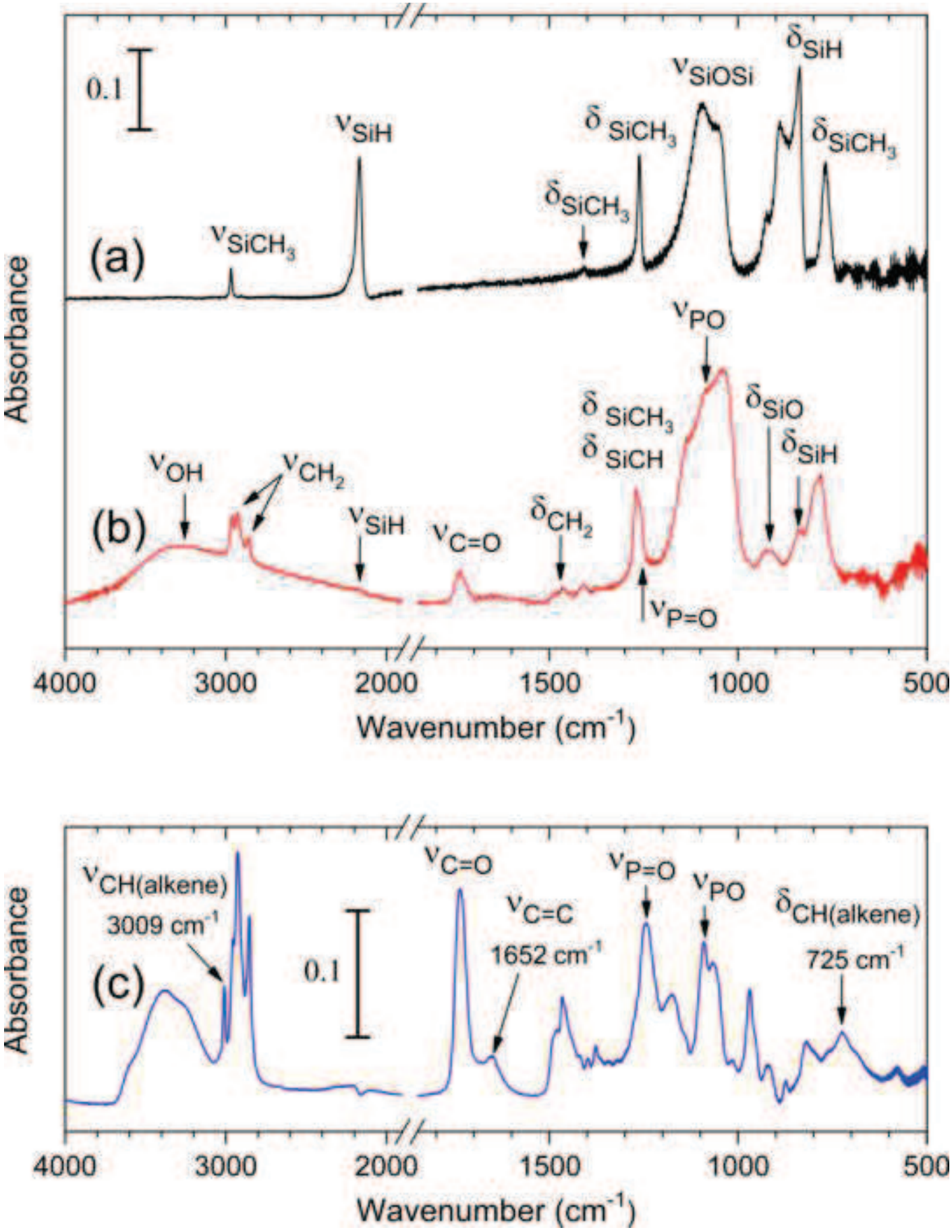

Fig. 2

Click here to download high resolution image

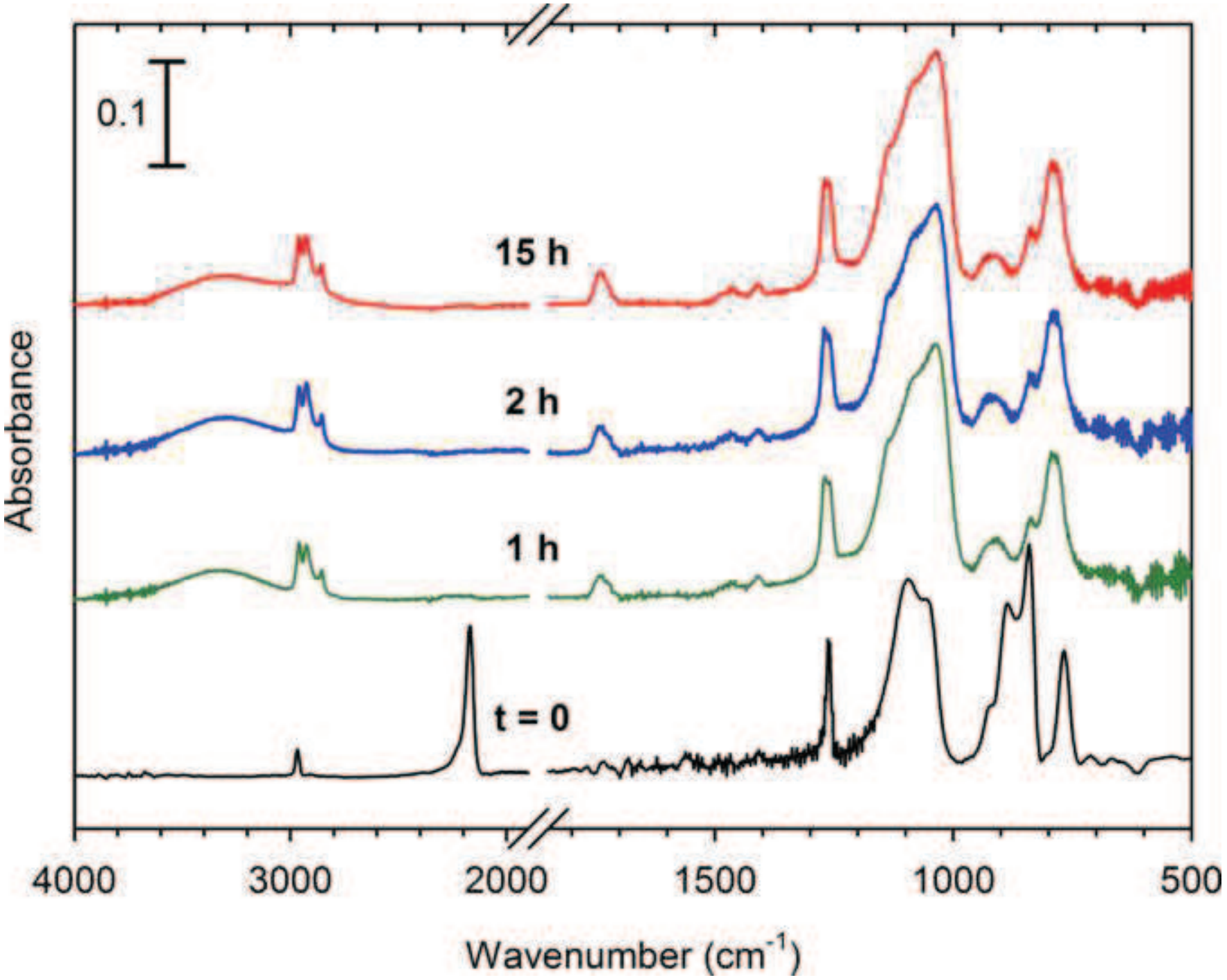

Fig. 3
Click here to download high resolution image

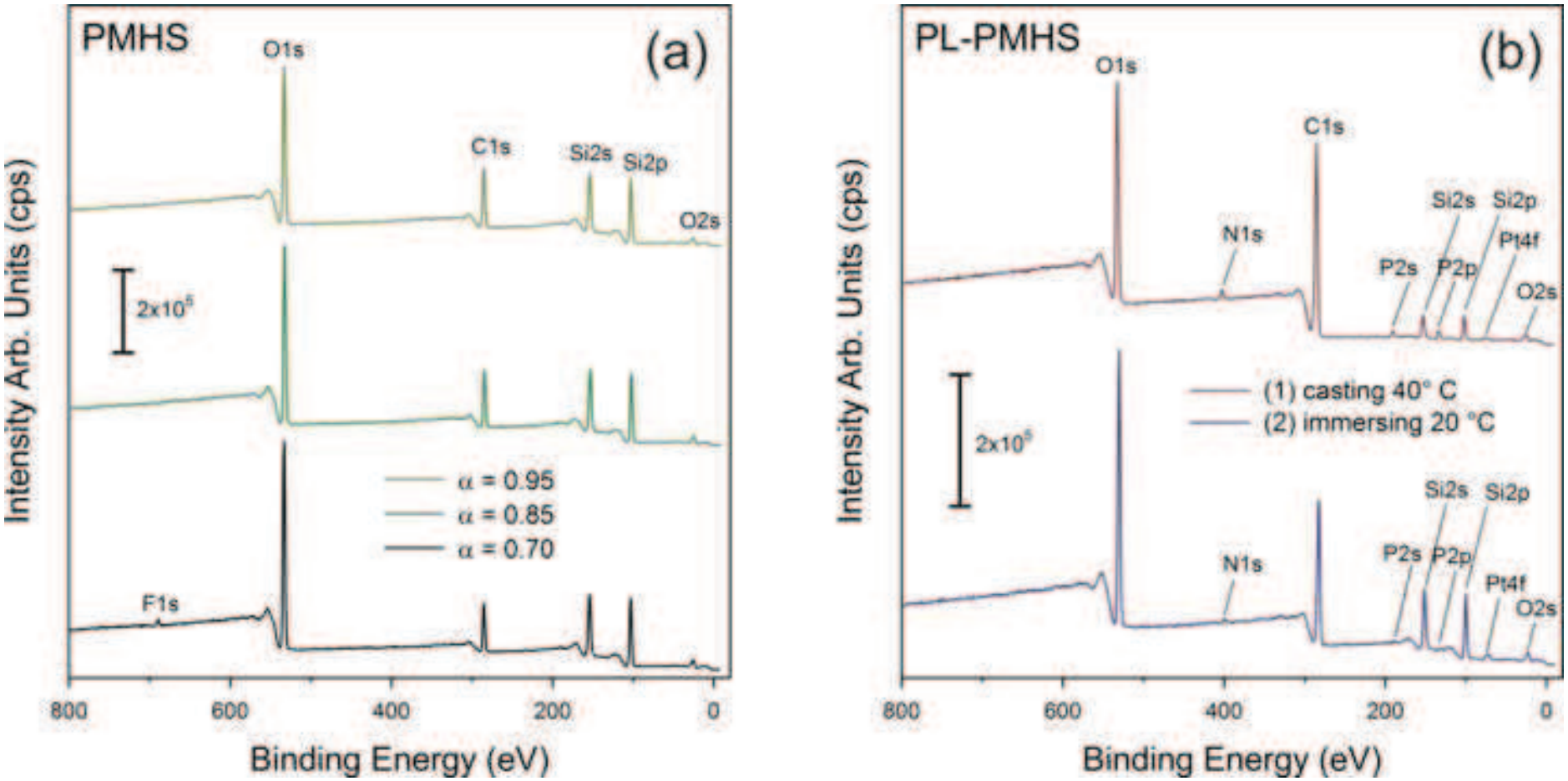

Fig. 4

Click here to download high resolution image

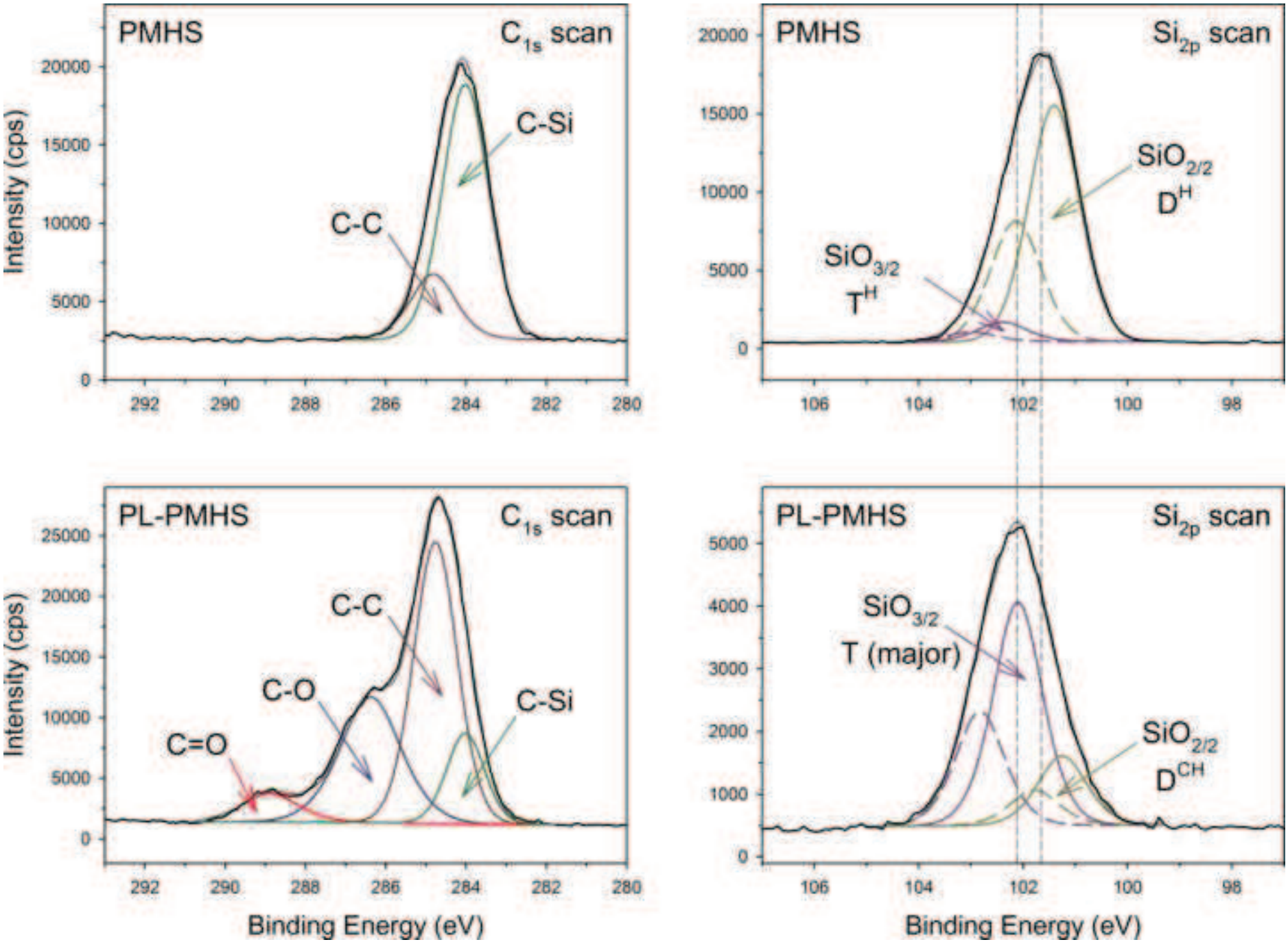

Fig. 5
Click here to download high resolution image

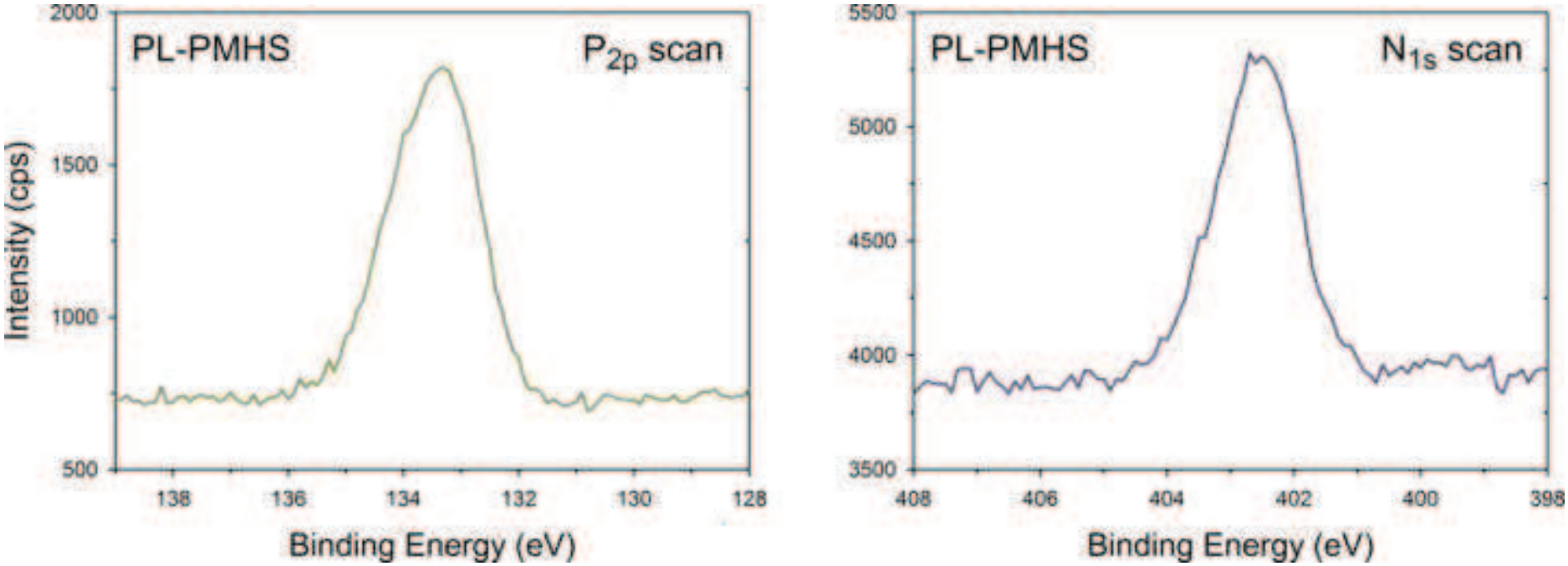

Fig. 6
Click here to download high resolution image

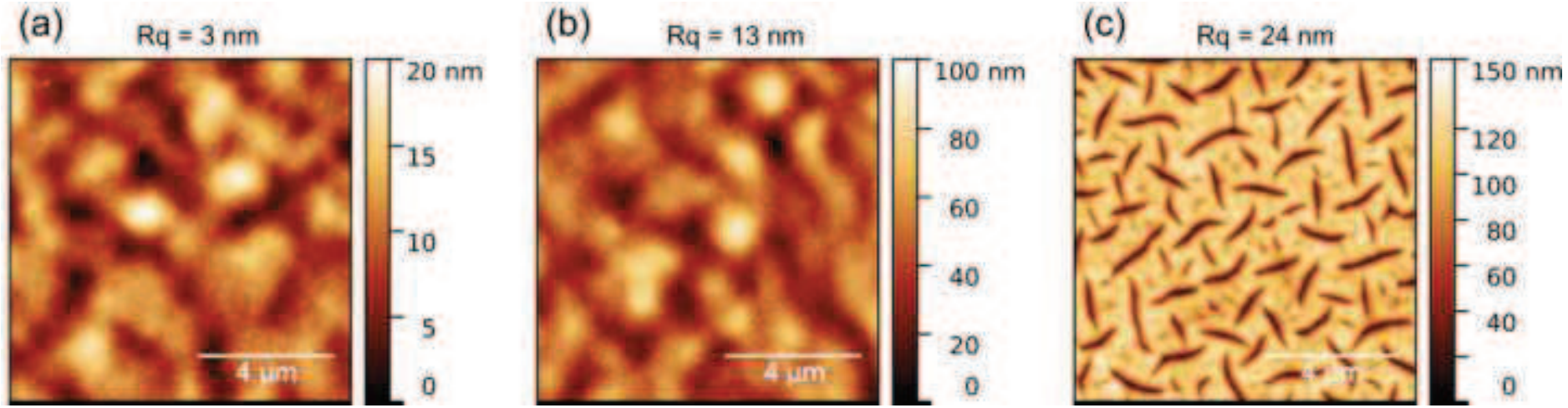

Fig. 7
Click here to download high resolution image

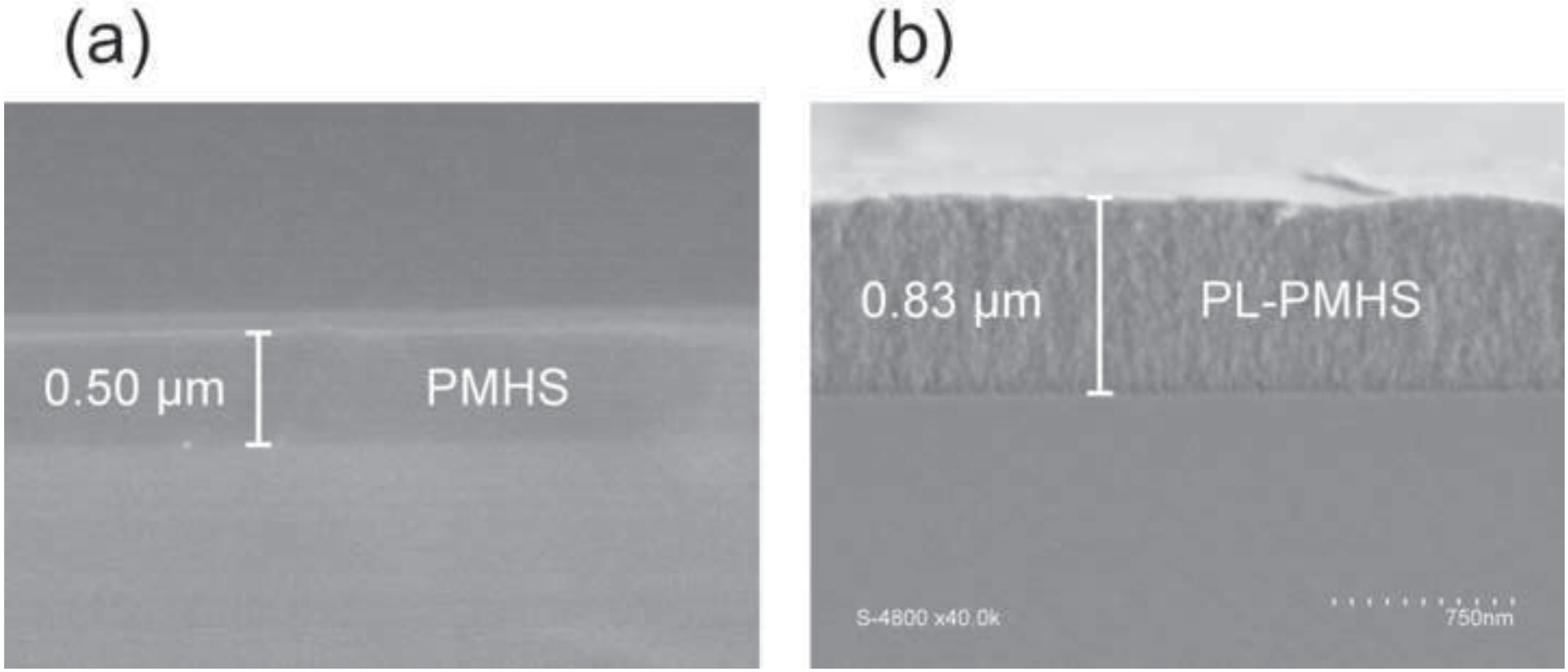

Fig. 8
Click here to download high resolution image